ANNEXURE

Introduction

Recent developments in designing surface functionalized mesoporous silica nanoparticles (MSNs) have gain much interaction in the field of drug delivery. As release kinetics of drug from the pores mainly depend on pore size [1], molecular size of the drug [2] and the drug–surface interaction, which can be done by functionalizing surface of mesoporous silica nanoparticles by proper functional group to increase drug–surface interaction. Further, they have properties like higher surface area, ordered porosity, higher adsorption capacity, biocompatibility, non-cytotoxicity [3, 4], effective cellular uptake [5] and possibility of drug loading [6], they have been effectively explored as drug delivery carrier. Due to this extra ordinary property, in mesoporous silica nanoparticles, drug molecules are effortlessly absorbed by simple diffusion mechanisms without affecting the chemical nature of the nanoparticles.

History of MCM-41 type MSNs as carrier

1. In 2004, Victor S.-Y. Lin and his group have reported Polyamidoamine Dendrimer-Capped MCM-41 type mesoporous silica nanoparticles and study as Gene Transfection Reagent [7].
2. In 2005, same group have studied the release of Adenosine 5-Triphosphate from MCM-41 type mesoporous silica nanoparticles which was functionalized by poly(amido amine) dendrimers [8]. In 2006, same group have further reported functionalization of MCM-41 type mesoporous silica nanoparticles by 3-aminopropyl (AP), N-(2-aminoethyl)-3-aminopropyl (AEAP), and N-folate-3-aminopropyl group. They have investigated the mechanism and efficiency of endocytosis of these materials with different charge profiles on human cervical cancer cells (HeLa) [9]. In 2007, same group have further reported the in vitro uptake and release of cytochrome C from MCM-41 type mesoporous silica nanoparticles [10]. In the same year, J.I. Zink and his group have reported release study of anticancer drug, Camptothecin from mesoporous silica nanoparticle (MCM-41) [11].
3. In 2008, Mou et al have reported functionalization of MCM-41 type mesoporous silica nanoparticles by trimethylammonium group and studied the in vitro release of Orange II (a fluorescent tracing molecule), and sulfasalazine (an anti-inflammatory prod-rug used for bowel disease) [12]. V. S.-Y. Lin et al have reported the gene delivery using MCM-41 type mesoporous silica nanoparticle [13].
4. In 2009, Wang et al have reported synthesis of MCM-41 type mesoporous silsica nanoparticles and functionalization of it using Polyelectrolyte multilayers (PEM) to prevent the premature leakage of doxorubicin [14]. During the same year, V. S.-Y. Lin

et al have reported glucose responsive release of insulin and cyclic AMP using MCM-41 type mesoporous silica nanoparticles [15].

5. In 2010, Martnez Manez et al have reported functionalization of MCM-41 type mesoporous silica nanoparticles after loading of fluorescein by 3-aminopropyl group and studied the release of fluorescein [16].
6. In 2011, Ebeid et al have reported synthesis of three types of mesoporous materials: pure mesoporous silica (MCM-41), a Nano composite of mesoporous silica with hydroxyapatite (MCM-41-HA) and mesoporous silica/gold Nano rods Nano composite (MCM-41-GNRs) and used these as carrier for coumarin [17]. Shunai Che et al have reported pH responsive delivery of mitoxantrone from MCM-41 type mesoporous silica nanoparticles by varying the electrostatic interaction between negatively charged silicate and positively charged MX under designed pH4.0-7.4 in PBS solution [18].
7. In 2012, Perona et al have reported release study of Rhodamine B loaded into MCM-41 nanoparticle functionalized by oligosaccharide [19]. Martınez Maenez et al have reported Amidase-responsive controlled release of Camptothecin from gluconamide-capped MCM-41 nanoparticles [20]. Zhao et al have reported functionalization of MCM-41 nanoparticle by amino-β-cyclodextrin ring and studied the release profile of Doxorubicin [21].
8. In 2013, Yoncheva et al have reported Indometacin loading and in vitro release from carbopol coated MCM-41 nanoparticles [22]. Gaberscek et al have reported release of fluorescein disodium salt and carboxyfluorescein from MCM-41 nanoparticles functionalized by Poly(propylene imine) dendrimer [23]. Jalil et al have reported controlled release of ibuprofen from MCM-41 nanoparticles functionlized by 3-aminopropyl group [R24]. Krishnan et al have reported in vitro release of 5-fluorouracil using MCM-41 nanoparticle functionalized by 3-mercaptopropyl group [25].
9. In 2014, Popova et al have reported functionalization of MCM-41 nanoparticle by post-synthesis method with amino and carboxylic groups. They have studied the release profile of mesalazine using these functionalized nanoparticles [26]. Chang-Sik Ha et al have reported functionalization of MCM-41 nanoparticle by a hydrophobic group, N-3-(trimethoxysilyl)propyl aniline and used as carrier for 5-fluorouracil and famotidine [27]. Tehrani and Pourjavadi have reported release of Erythromycin from MCM-41 nanoparticle Coated by PEGylated Chitosan [28]. Zendehdel et al have reported controlled release of Etronidazole from MCM-41 nanoparticle functionalized by poly ethylene glycol [29].
10. In 2017, Cheng et al have reported functionalization of MCM-41 nanoparticle by β-cyclodextrin with imine bond and azobenzene derivative and studied the release of

tris(2,2′-bipyridyl)ruthenium(II) chloride hexahydrate [30]. Cao Li et al have reported in vitro release of Doxorubicin from MCM-41 nanoparticle functionalized by pH-sensitive dextran [31].

11. Nhavene et al. have reported controlled release of benznidazol for Chagas diseases treatment using MCM-41 nanoparticle [32].
12. Tzankov and his group have reported controlled release of pramipexole using MCM-41 nanoparticle functionalized by chitosan [33].

Hence, the literature survey displays that MCM-41 type mesoporous silica has been widely used as carriers (to deliver large number of drug molecules) with or without functionalization by organic moieties. Present work describes functionalization of MCM-41 type mesoporous silica nanoparticles using 12-tungstophosphoric acid and studied it as carrier for in vitro release of L-Arginine, Aspirin and Captopril.

References

[1] D. Zhao, J. Feng, Q. Huo, N. Melosh, G.H. Fredricwkson, B.F. Chmelka, G.D. Stucky, Science 279, 548 (1998).

[2] Y. Han, D. Li, L. Zhao, F.-S. Xiao, Angew. Chem. Int. Ed. 42, 3633 (2003).

[3] W.S. Lin, W.Y. Huang, X.D. Zhou, Y.F. Ma, Toxicol. Appl. Pharmacol. 217, 252 (2006).

[4] R. Wottrich, S. Diabate, H.F. Krug, Int. J. Hyg. Envir. Heal. 207, 353 (2004).

[5] V.P. Torchilin, Nat Rev Drug Discov., 4, 145 (2005).

[6] L. Tang, T.M. Fan, L.B. Borst, J. Cheng, Acs. Nano. 6, 3954 (2012).

[7] R. Daniela, R. Radu, C-Y. Lai, K. Jeftinija, E.W. Rowe, S. Jeftinija, V. S.-Y. Lin, J. Am. Chem. Soc.126, 13216 (2004).

[8] J.A. Gruenhagen, C-YU Lai, D.R. Radu, V. S.-Y. LIN, E.S. Yeung, Appl. Spectro., 59, 424 (2005).

[9] I. Slowing, B.G. Trewyn, V. S.-Y. Lin, J. Am. Cchem. Soc., 128, 14792 (2006).

[10] I.I. Slowing, B.G. Trewyn, V. S.-Y. Lin, J. Am. Chem. Soc., 129, 8845 (2007).

[11] J. Lu, M. Liong, J.I. Zink, F. Tamanoi, Small, 3, 8, 1341 (2007).

[12] C-H. Lee, L-W. Lo, C-Y. Mou, C-S. Yang, Adv. Funct. Mater. 18, 3283 (2008).

[13] I.I. Slowing, J.L. Vivero-Escoto, C-W. Wu, V. S.-Y. Lin, Adv. Drug Deliv. Rev., 60, 1278 (2008).

[14] C-L. Zhu, X-Y. Song, W-H. Zhou, H-H. Yang, Y-H. Wenb, X-R. Wang, J. Mater. Chem., 19, 7765 (2009).

[15] Y. Zhao, B.G. Trewyn, I.I. Slowing, V. S.-Y. Lin, J. Am. Chem. Soc. 131, 8398 (2009).

[16] E. Climent, R. Martnez-Manez, F. Sancen, M.D. Marcos, J. Soto, A. Maquieira, P. Amors, Angew. Chem. Int. Ed., 49, 7281 (2010).

[17] A.S. Al-Kady, M. Gaber, M.M. Hussein, El-Z.M. Ebeid, Eur. J. Pharm. Biopharma., 77, 66 (2011).

[18] Y. Ma, Z. Lin, H. Zheng, L. Xing, C. Li, J. Cui, S. Che, J. Mater. Chem., 21, 9483 (2011).

[19] A. Agostini, L. Mondragn, A. Bernardos, R. Martnez-MÇez, M.D. Marcos, F. Sancenn, J. Soto, A. Costero, C. Manguan-arca, R. Perona, M. Moreno-Torres, R. Aparicio-Sanchis, J. Murgu, Angew. Chem. Int. Ed., 51, 1 (2012).

[20] I. Candel, E. Aznar, L. Mondragon, C. de la Torre, R. Martınez-Ma-nez, F. Sancenon, M.D. Marcos, P. Amoros, C. Guillem, E. Perez-Pay, A. Costero, S. Gilad, M. Parra, Nanoscale, 4, 7237 (2012).

[21] Q. Zhang, F. Liu, K.T. Nguyen, X. Ma, X. Wang, B. Xing, Y. Zhao, Adv. Funct. Mater, 22, 5144 (2012).

[22] B. Tzankov, K. Yoncheva, M. Popova, A. Szegedi, G. Momekov, J. Mihály, N. Lambov, Microporous Mesoporous Materials 171, 131 (2013).

[23] P. Nadrah, F. Porta, O. Planinsek, A. Krosb, M. Gaberscek, Phys. Chem. Chem. Phys., 15, 10740 (2013).

[24] N.H.N. Kamarudin, A.A. Jalil, S. Triwahyono, N.F.M. Salleh, A.H. Karim, R.R. Mukti, B.H. Hameed, A. Ahmad, Microporous Mesoporous Materials 180, 235 (2013).

[25] B. Murugan, L.N. Ramana, S. Gandhi, S. Sethuraman, U. M. Krishnan, J. Mater. Chem. B, 1, 3494 (2013).

[26] M. Popova, A. Szegedi, K. Yoncheva, S. Konstantinov, G.P. Petrova, H.A. Aleksandrov, G.N. Vayssilov, P. Shestakova, Microporous Mesoporous Materials 198, 247 (2014).

[27] A. Mathew, S. Parambadath, S.S. Park, C-S. Ha, Microporous Mesoporous Materials 200, 124 (2014).

[28] A. Pourjavadi, Z.M. Tehrani, I. J. Polymeric Mater. Polymeric Biomater. 63, 692 (2014).

[29] M. Zendehdel, G. Cruciani, F.S. Kar, A. Barati, J. Environ. Health Sci. Eng. 12, 35 (2014).

[30] J. Zhao, Z. He, B. Li, T. Cheng, G. Liu, Mater. Sci. Eng. C 73, 1 (2017).

[31] M. Zhanga, J. Liub, Y. Kuangc, Q. Lib, D-W. Zhenga, Q. Songa, H. Chena, X. Chena, Y. Xud, C. Li, B. Jiang, International Journal of Biological Macromolecules, 98, 691 (2017).

[32] E.P.F. Nhavene, W.M. da Silva, R.R. Trivelato J, P.L. Gastelois, T. Venâncio, R. N. Ronaldo J.C. Baptista, C.R. Machado, W.A. de Almeida Macedo, E.M.B. de Sousa, microporous mesoporous mater, 272, 265 (2018).

[33] B. Tzankov, V. Tzankova, D. Aluani, Y. Yordanov, I. Spassova, D. Kovacheva, K. Avramova, M. Valoti, K. Yoncheva, J Drug. Deli. Sci. Technol. 51, 26 (2019)

Part A

In vitro release study of L-arginine from Np-MCM-41 and TPA-Np-MCM-41

J Porous Mater (2016) 23:1113–1123
DOI 10.1007/s10934-016-0169-0

12-Tungstophosphoric acid functionalized MCM-41: synthesis, characterization and study of controlled in vitro release of L-arginine

Anjali Patel[1] · **Priyanka Solanki**[1]

Published online: 31 March 2016

Abstract The present paper consists of functionalization of MCM-41 by 12-tungstophosphoric acid (TPA), loading of L-arginine onto the functionalized MCM-41 and characterization of both loaded and unloaded functionalized MCM-41 using various physicochemical techniques. The in vitro release study of L-arginine from functionalized MCM-41 was carried out in simulated body fluid at room temperature under stirring as well as under static condition. The study shows that the presence of TPA strongly influences the release rate of L-arginine. A study on release mechanism and release kinetics was also carried out using Higuchi model and first order release kinetic model.

Keywords MCM-41 · 12-Tungstophosphoric acid · L-Arginine · In vitro release · Release kinetics · Release mechanism

1 Introduction

Recently, research has been focused on the application of mesoporous silica, mainly MCM-41 as potential drug delivery system because of its unique property such as ordered porosity at mesoscale, high specific surface area, and higher adsorption capacity, presence of surface Si–OH group, biocompatibility and non-toxicity [1, 2]. In ordered mesoporous silica materials, drug molecules are easily absorbed by simple diffusion mechanisms without affecting the chemical nature of the silica on the pore walls.

✉ Anjali Patel
aupatel_chem@yahoo.com

[1] Department of Chemistry, Faculty of Science, The M. S. University of Baroda, Vadodara, Gujarat 390002, India

Release kinetics of drug from the pores mainly depend on pore size [3], molecular size of the drug [4] and the drug–surface interaction, which can be done by functionalizing surface of mesoporous silica by proper functional group to increase drug–surface interaction. The later one is the most develop method to control drug delivery.

In 2003, first time Vallet-Regi et al. [5] have reported functionalisation of MCM-41 by aminopropyl group and studied the release of ibuprofen. In 2008, same group has reported amino functionalized MCM-41 and studied the effect of functionalization on adsorption of ibuprofen as well as release rate of the same. The result showed that the higher adsorption capacity as well as controlled release of ibuprofen was found for functionalized MCM-41 compare to unfunctionalized MCM-41 [6]. Szegedi et al. [7] have synthesized MCM-41 functionalized by amino group and studied the release profile of ibuprofen from the same. Yoncheva et al. [8] have reported the release profile of cis-platin from MCM-41 functionalized with carboxylic group and show the effect of functionalization on release profile of cis-platin. In 2010, Li et al. [9] have synthesized MCM-41 which was functionalized by 3-aminopropyl group and 3-chloropropyl group and L-tryptophane and used amoxicillin as model drug. The slower release rate was observed for the same system. Also, Tang et al. [10] synthesized dimethylsilyl (DMS) modified MCM-41 and use as drug carrier for the release study of ibuprofen. In 2011, Sun et al. [11] have reported the controlled release of aspirin from MCM-41, functionalized with 3-aminopropyl group. In 2012, Zhu et al. [12] have reported amino functionalized MCM-41 and studied the release of heparin. In the same year, Maria et al. [13] have investigated the release profile of Cephalosporin from MCM-41 functionalized with 3-aminopropyl group and tri-ethoxyvinyl group. The effect of amino functionalized MCM-41 on release profile of

Advanced Porous Materials
Vol. 6, 80–88, 2018

L-Arginine Encapsulated Mesoporous MCM-41 Nanoparticles: A Study on *In Vitro* Release as Well as Kinetics

Priyanka Solanki and Anjali Patel*

Department of Chemistry, Faculty of Science, The Maharaja Sayajirao University of Baroda, Vadodara 390002, Gujarat, India

The present article describes encapsulation of L-arginine into mesoporous MCM-41 nanoparticle having average particle size ~53 nm, by wet impregnation method, characterization by various physicochemical techniques and *in vitro* controlled release of L-arginine in simulated body fluid at room temperature as well as at body temperature (37 °C) under stirring condition. It was found that MCM-41 was able to release L-arginine in a controlled manner and almost same release of L-arginine was observed, in both cases. After that a slow and delayed release was observed and reached to 80% up to 28 h. Further, a study was also carried out using First order release kinetic Model as well as Higuchi Model to understand the mechanism.

Keywords: L-Arginine, MCM-41 Nanoparticle, *In Vitro* Release, Kinetics, Mechanism.

1. INTRODUCTION

L-arginine is a semi essential amino acid, a substrate for the synthesis of nitric oxide (NO), polyamines and agmatine. It influence hormonal release and also involved in the synthesis of pyrimidine bases.[1–4] It is the main source of generation of NO via NO synthase (NOS). The 3 NOS isoforms have been found to be expressed in the kidney.[4] In the kidney endothelial NOS is important in the maintenance of glomerular filtration rate, regional vascular tone, and renal blood flow. The neuronal NOS (nNOS) is expressed primarily in the macula-densa and participates in the control of glomerular hemodynamic and rennin release. The inducible (iNOS) is expressed in the kidney under pathological condition in the glomerular mesangium, infiltrating macrophages and tubules.[5] L-arginine is the substrate for arginases, a group of enzyme that are involved in tissue repair processes and that metabolize L-arginine to l-ornithine.[6] It is also a precursor for polyamine synthesis which is also involved in tissue repair and wound healing.[7–8] During the time of stress, body does not provide sufficient amount of L-arginine for metabolic needs. Hence under this condition, L-arginine supplementation has been considered as an adjunct treatment for restoring normal function.[7,9–10] It was also found that compared to oral administration, intravenous administration of L-arginine to the patients with coronary artery disease increases the bioavailability of vascular nitric oxide (NO) which shows the vasodilator effect. Further it was found that in case of oral administration, the bio-availability of L-arginine decreases as it is utilized by arginase for the production of urea and ornithine and thus competes with NO synthase for substrate availability,[1,11] 40% L-Arginine is degraded in the intestine by arginase.[12] The mentioned problem can be overcome if some carrier will be used. The advantage of using carrier is that it can provide sufficient amount of L-arginine for NO production by a controlled release.

Thus, even though, L-arginine is important and is used as drug under certain conditions, very few reports are available. Qiang Gao et al. have reported the adsorption of L-arginine on SBA-15 at different pH.[13] Lacasta et al. have reported synthesis of chiral ordered mesoporous silica in presence of L-arginine and different amino acid to induce chirality in mesoporous silica and use it for chiral resolution.[14] Diaz et al., have reported immobilization of trypsin into MCM-41 which was active for the hydrolysis of N-a-benzoyl-DL-arginine-4-nitroanibde (BAPNA).[15] Casado et al. have reported synthesis of chiral ordered mesoporous silica in the presence of amino acid proline by combining tetraethyl orthosilicate and quaternized aminosilane silica sources for resolution of proline racemate.[16] However, no report is available on controlled release of L-arginine. Mesoporous materials are well known for its unique features such as high surface area, large pore size and large pore volume.[17,18] Mesoporous silica nanoparticles (MSNs) especially, have been

*Author to whom correspondence should be addressed.

2327-3941/2018/6/080/009 doi:10.1166/apm.2018.1156

In vitro controlled release of L-Arginine from MCM-41

Experimental

Synthesis of mesoporous nanoparticle

Mesoporous nanoparticle was synthesized using reported procedure with slight modification [1]. The Surfactant (CTAB) was added to the very dilute solution of NaOH with stirring. When the solution became homogeneous, TEOS was added drop wise and the obtained gel was aged for 2 h at 60 ^{o}C. The resulting product was filtered, washed with distilled water, dried at room temperature and was calcined at 555 ^{o}C in air for 5 h. The obtained material was designated as Np-MCM-41.

Loading of L-Arginine into Np-MCM-41

A series of materials containing L-Arginine (10%-30%) on Np-MCM-41were synthesized using wet impregnation method. 0.1 g of L-Arginine in 10 ml distilled water gives 10% solution. 1 g of Np-MCM-41 was impregnated with this solution and dried at 100 ^{o}C for 5 h. The obtained material was designated as L-arg$_1$/Np-MCM-41. Likewise 20% and 30% L-Arginine loaded Np-MCM-41 was prepared and designated as L-arg$_2$/Np-MCM-41 and L-arg$_3$/Np-MCM-41 respectively.

Characterizations

The BET surface area measurements were performed in a Micromeritics ASAP 2010 volumetric static adsorption instrument with N_2 adsorption at 77 K. The pore size distributions were calculated by BJH adsorption-desorption method. Degassing condition for analysis was as follows: 1. temperature: phase (i): 60 ^{o}C, Phase (ii): 90 ^{o}C; 2. Time: 400 min. TEM analysis was carried out on JEOL (JAPAN) TEM instrument (model-JEM 100CX II) with accelerating voltage of 200 kV. The samples were dispersed in ethanol and ultrasonicated for 5-10 min. A small drop of the sample was then taken in a carbon coated copper grid and dried before viewing. TGA of the Np-MCM-14 and L-Arginine loaded Np-MCM-41 were carried out using a Mettler Toledo Star SW 7.01 instrument under nitrogen atmosphere from 30 to 570 ^{o}C at the heating rate of 10 ^{o}C/min. The FTIR spectra of pure Np-MCM-41 and L-Arginine loaded Np-MCM-41 were obtained by using KBr palate on Perkin Elmer instrument. The IR spectra, in absorbance mode, were obtained over the spectral region 400 to 4000

cm^{-1}. The XRD pattern was obtained by using PHILIPS PW-1830. The conditions were: Cu Kα radiation (1.54 A^o), scanning angle from 0^o to 10^o. The ^{29}Si NMR spectra were recorded at Mercury Plus 300 MHz using a 5 mm Dual Broad Band rotor probe with TMS as an external standard.

In vitro release study of L-Arginine from Np-MCM-41

The in vitro L-Arginine release profile was obtained by soaking 0.5 g L-arg_1/Np-MCM-41 in 62.5 ml of SBF at room temperature and at 200 rpm. The L-Arginine concentration in release fluid at pH 7.4 for the different release time was determined using (Systronic) UV-Vis spectrophotometer at 570 nm. In each case, 0.5 ml of release fluid were taken out for analysis of the L-Arginine concentration and equal amount of fresh SBF was added to the release system to maintain constant volume. Likewise, the release profile of L-arg_2/Np-MCM-41 and L-arg_3/Np-MCM-41 was obtained by soaking 0.6 g of L-arg_2/Np-MCM-41 and 0.4 g of L-arg_3/Np-MCM-41 in 150 ml of SBF. Each analysis was carried out three times and the associated percentage release values of L-Arginine were found in the range of ±1%.

To know the complete mass balance the amount of remaining L-Arginine in porous solid (after release experiment), the remaining residue was filter and then mixed with ethanol. The mixture was stirred for 10 h, at room temperature. After that the mixture was filtered and washes with ethanol. The filtrate was analyzed for remaining L-Arginine content using same method as stated earlier.

Results and Discussion

Characterizations

Nitrogen adsorption-desorption isotherm

The nitrogen adsorption-desorption isotherms of a) Np-MCM-41, b) Larg$_1$/Np-MCM-41, c) L-arg$_2$/Np-MCM-41 and L-arg$_3$/Np-MCM-41 are shown in Figure 1 and data are presented in Table 1. It is seen from the Table 1 that with increasing % loading of L-Arginine, there is a drastic decrease in surface area and pore volume is observed as compared to that of pure Np-MCM-41 (Table 1). This is the first indication of encapsulation of L-Arginine into the mesoporous channel as well as presence of interaction between Np-MCM-41 and L-Arginine. The significant decrease in surface area and pore for L-arg$_2$/Np-MCM-41 and L-arg$_3$/Np-MCM-41 indicates filling of all the channels by multi-layered adsorption of L-Arginine into the Np-MCM-41 which may causes the collapse of mesoporous structure. This is also observed in the adsorption-desorption isotherms (Figure 1).

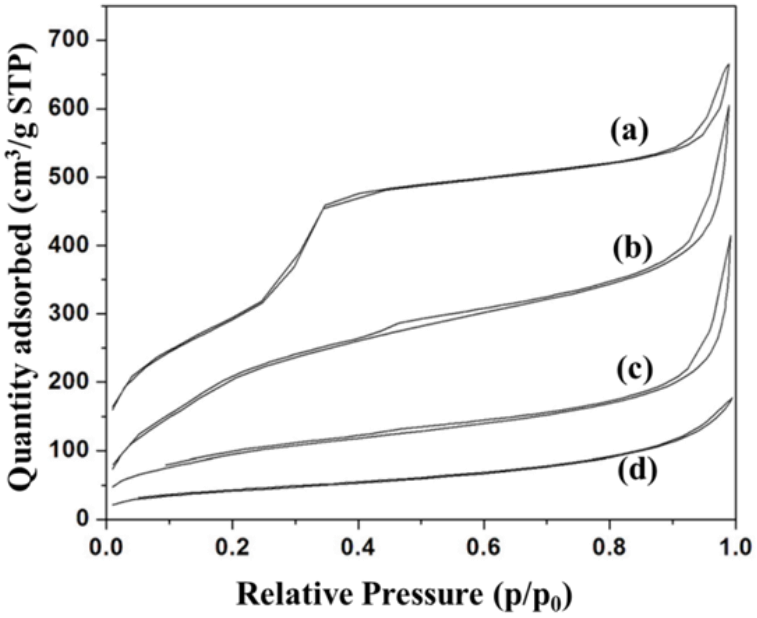

Figure 1. N_2 adsorption-desorption isotherm of a) Np-MCM-41, b) L-arg$_1$/Np-MCM-41, c) L-arg$_2$/Np-MCM-41 and d) L-arg$_3$/Np-MCM-41

The nitrogen adsorption-desorption isotherm of Np-MCM-41 is of type IV in nature with H1 hysteresis loop, according to the IUPAC classification is a characteristic of mesoporous solids. The adsorption branch of each isotherm showed a sharp inflection indicates a typical capillary condensation within uniform pores. The L-

arg_1/Np-MCM-41 show type (IV) pattern with three stages: monolayer adsorption of nitrogen on the walls of mesopores ($P/P_0 < 0.4$), the part characterized by a steep increase in adsorption due to capillary condensation in mesopores with hysteresis ($P/P_0 = 0.45\text{-}0.6$), and multi-layered adsorption on the outer surface of the particle. However slight deviation in the isotherm of L-arg_2/Np-MCM-41 and L-arg_3/Np-MCM-41 may be due to the collapse of some mesopores and multi-layered adsorption of L-Arginine into Np-MCM-41. Based on the study, L-arg_1/Np-MCM-41 was selected for detailed study.

Table 1: Structure parameters of loaded and unloaded Np-MCM-41

Materials	**Specific surface area (m^2/g)**	**Pore volume (cm^3/g)**
Np-MCM-41	1100.0	1.06
L-arg_1/Np-MCM-41	478.0	0.44
L-arg_2/Np-MCM-41	191.9	0.32
L-arg_3/Np-MCM-41	54.1	0.09

TEM

TEM images of Np-MCM-41 and L-arg_1/Np-MCM-41 are shown in Figure 2, in both cases, TEM images confirming the presence of well-ordered hexagonal arrays of channels. It also shows mono-dispersed spherical morphology with the average particle size ~ 53 nm. Further, absence of any agglomeration confirmed the well dispersion of L-Arginine into the channels of Np-MCM-14 as well as retention of porous structure of Np-MCM-41 even after the insertion of L-Arginine.

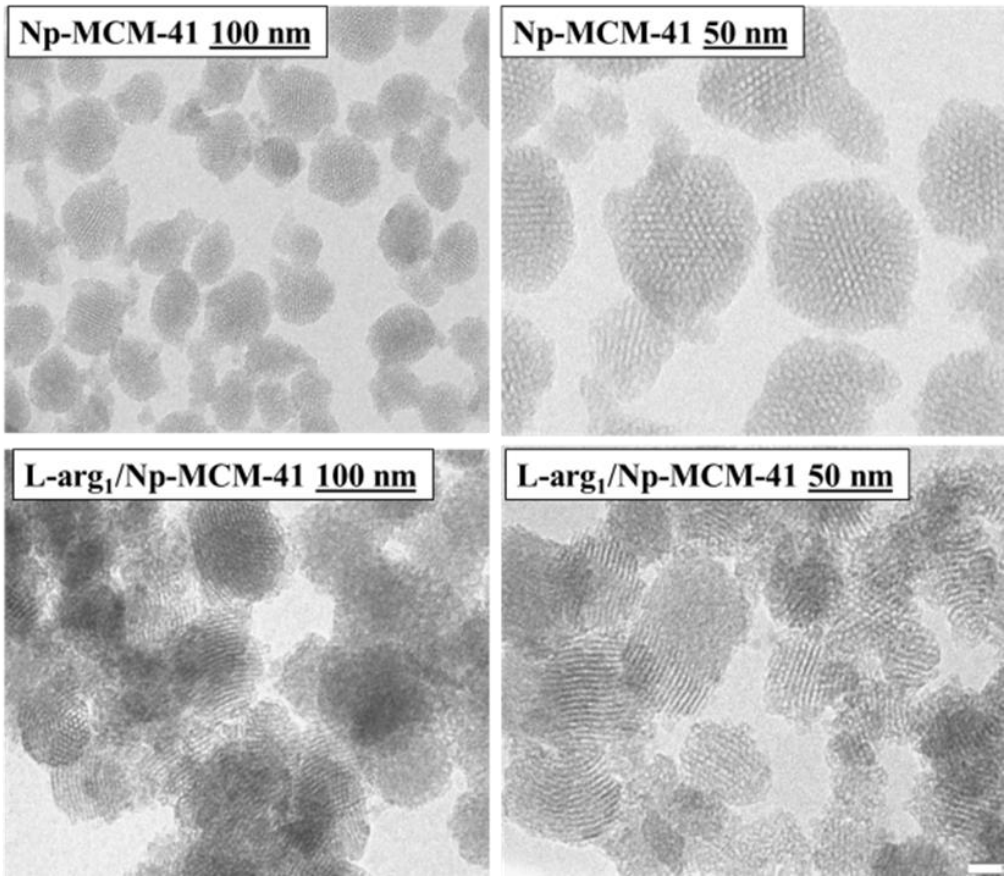

Figure 2. TEM images of Np-MCM-41 and L-arg$_1$/Np-MCM-41 at 100 and 50 nm resolution

TGA

TGA curve of pure Np-MCM-41 and L-arg$_1$/Np-MCM-41 are shown in Figure 3. TGA of Np-MCM-41 shows initial weight loss of 2.7 % at 100 ^{o}C. This may be due to the loss of adsorbed water molecules. The final 4.83 % weight loss above 300 ^{o}C may be due to the condensation of silanol groups to form siloxane bonds. The TGA of L-arg$_1$/Np-MCM-41 shows initial weight loss of 7.1% at 100 ^{o}C due to the presence of adsorbed water. Further, 14.8% weight loss from 200 ^{o}C to 550 ^{o}C suggest the removal of L-Arginine from Np-MCM-41 as well as the condensation of silanol groups to form siloxane bonds. As stated earlier, 4.83% weight loss is observed for pure Np-MCM-41 above 300 ^{o}C and 14.8% weight loss observed in case of L-arg$_1$/Np-MCM-41 from 150 ^{o}C to 550 ^{o}C which suggests the presence of 10% L-Arginine into Np-MCM-41.

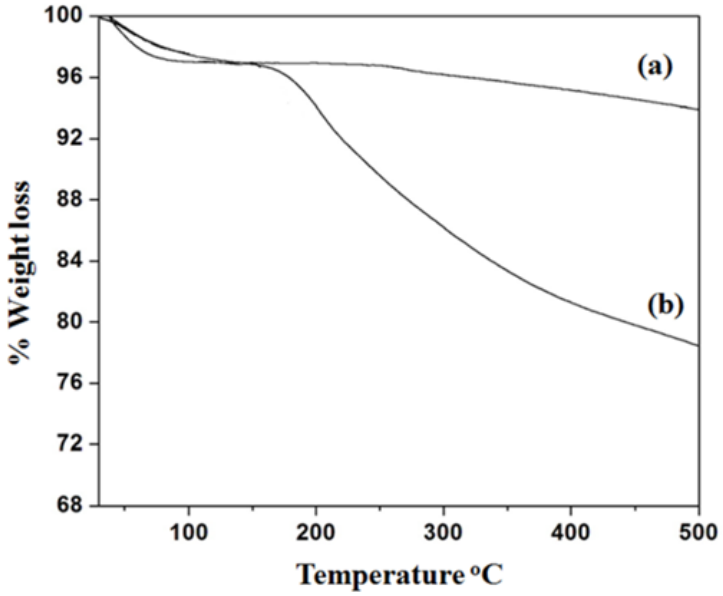

Figure 3. TGA patterns of (a) Np-MCM-41 and (b) L-arg$_1$/Np-MCM-41

FTIR

Figure 4 shows the FTIR spectra of (A) Np-MCM-41 and L-arg$_1$/Np-MCM-41; and (B) pure L-Arginine. FTIR spectra of Np-MCM-41 shows broad band around 1100-1300 cm^{-1} corresponds to asymmetric stretching of Si-O-Si. The band at 801cm^{-1} and 498 cm^{-1} are due to the stretching and bending vibration of Si-O-Si, respectively. The band at 3448 cm^{-1} was corresponds to stretching vibration of Si-OH. The FTIR spectrum of L-Arginine (Figure 5B) shows bands around 3151 cm^{-1}, 1680 cm^{-1}, 1574 cm^{-1} corresponds to N-H stretching vibration, NH_2 in plan bending vibration and C=O stretching vibration [2].

The FTIR spectra of L-arg$_1$/Np-MCM-41 shows additional vibration at 3185 cm^{-1}, 1696 cm^{-1} ,1668 cm^{-1} due to N-H stretching vibration, NH_2 in plan bending vibration and C-O stretching vibration. The band of Si-OH group in L-arg$_1$/Np-MCM-41 was shifted to 3364 cm^{-1}. Thus shifting of all bands are observed, however a significant shifting in C-O vibration band (1574 cm^{-1} to 1668 cm^{-1}) and in Si-OH stretching vibration band (3448 cm^{-1} to 3361 cm^{-1}) confirm the interaction between the carbonyl group of L-Arginine and Si-OH group of Np-MCM-41.

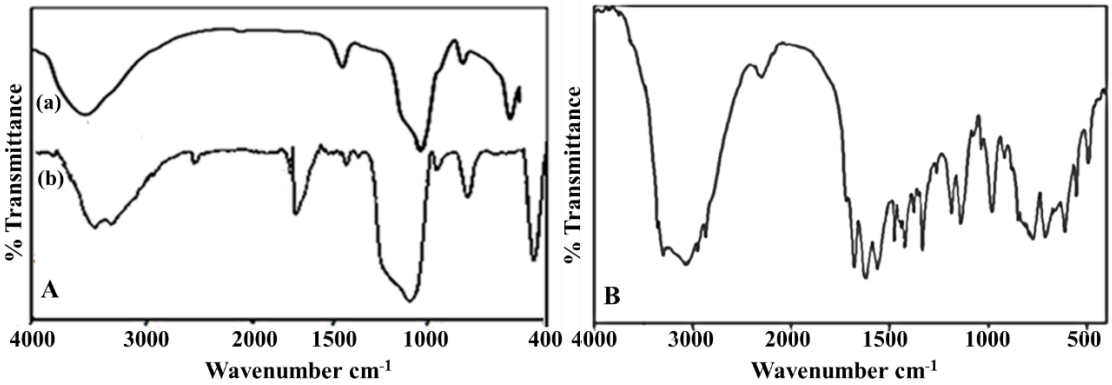

Figure 4. FTIR spectra of **A** (a) Np-MCM-41 and (b) L-arg$_1$/Np-MCM-41; **B** L-Arginine

Low angle powder XRD

Figure 5 shows low angle powder XRD of Np-MCM-41 and L-arg$_1$/Np-MCM-41. The low angle powder XRD of Np-MCM-41 displays an intense diffraction peak at 2θ = 2.43° which are assigned to the lattice faces (100), suggesting a hexagonal symmetry of Np-MCM-41. In addition to this weak peaks are observed at 2θ = 4.2-5.8° with very low intensity which are sometimes difficult to observed due to instrumental error [3]. Same observation for low angle powder XRD was reported by Zhu et al. [4] and Marand et al. [5]. Shifting as well as broadening in 2θ peak from 2.43^o to 1.8^o for L-arg$_1$/Np-MCM-41 may be due to L-Arginine insertion into the mesoporous channels of NP-MCM-41. The interaction between L-Arginine and Np-MCM-41 is further confirmed by ^{29}Si MAS NMR.

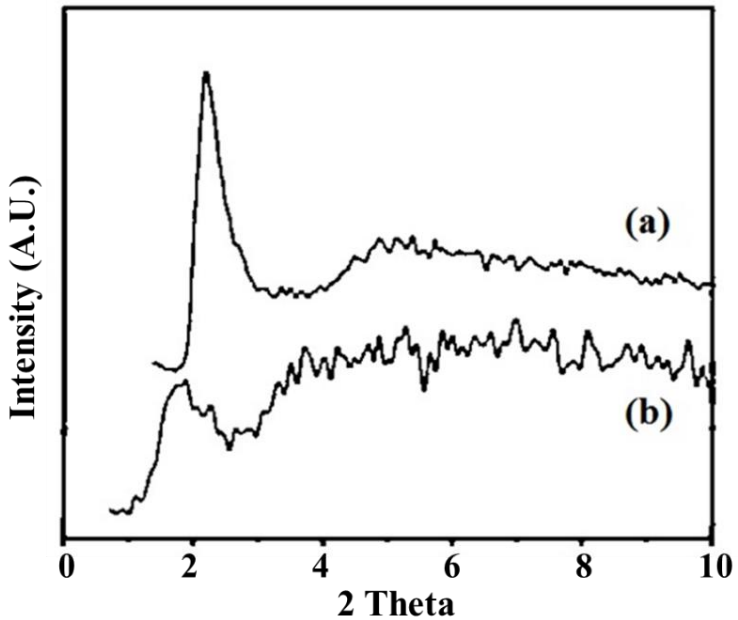

Figure 5. Powder XRD of (a) Np-MCM-41 and (b) L-arg$_1$/Np-MCM-41

In vitro L-Arginine release study from Np-MCM-41

The drug release study was carried out for all the three systems at physiological pH 7.4 using simulated body fluid under in vitro stirring conditions, at room temperature and the data are presented in Figure 6. The release profile shows the existence of two steps: (1) initial burst release and (2) fixed slow release. The initial burst release was started at 40%, 45% and 48% and was reached up to 55 %, 65 % and 56% for 10 h from L-arg$_1$/Np-MCM-41, L-arg$_2$/Np-MCM-41 and L-arg$_3$/Np-MCM-41, respectively.

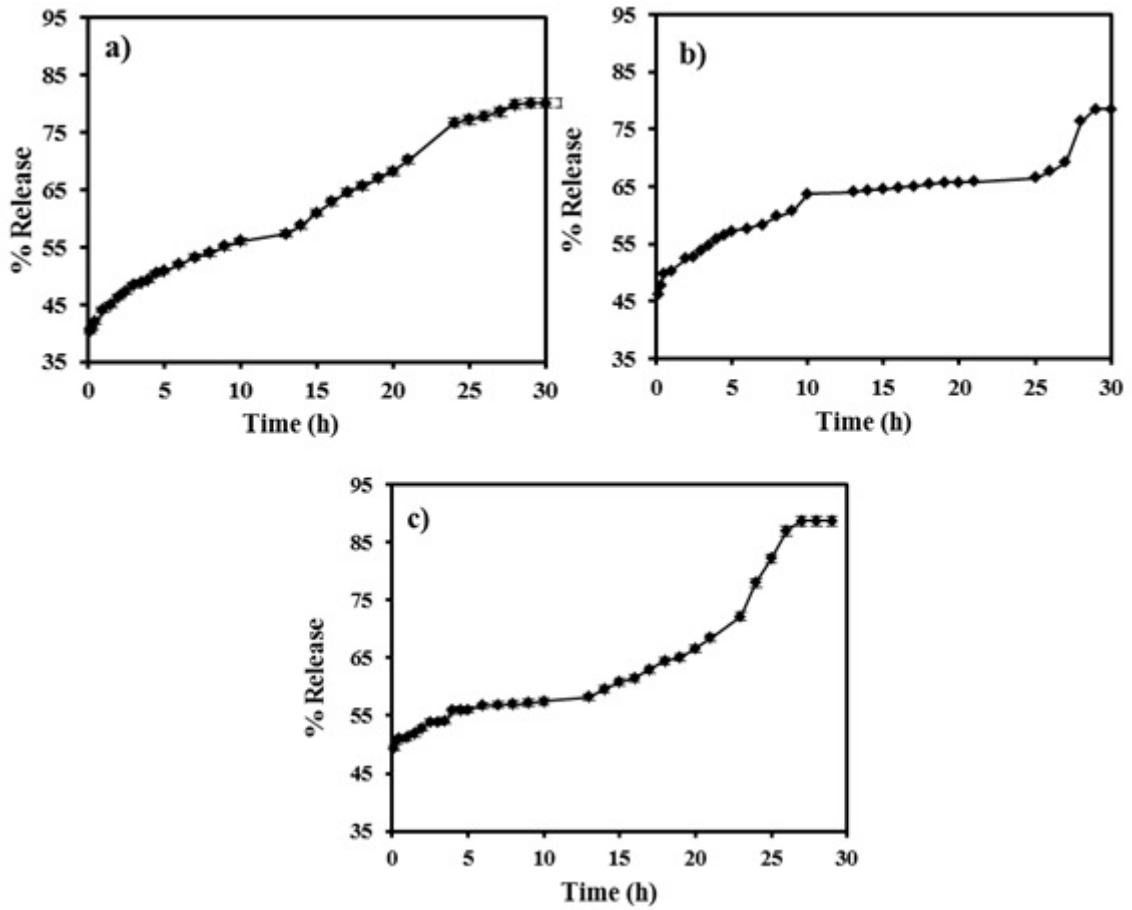

Figure 6. Release profile of a) L-arg$_1$/Np-MCM-41, b) L-arg$_2$/Np-MCM-41 and c) L-arg$_3$/Np-MCM-41 in SBF

The initial burst release was the result of dissolution of L-Arginine molecule adsorbed on the outer surface of Np-MCM-41, which indicates over loading of L-Arginine in later system which was also confirmed by BET analysis data. The second step involved fixed slow rate of release of L-Arginine molecule. This was reached up to 80% after 28 h and then it became constant. From the release percentage data it was found that more controlled release was observed for L-arg_1/Np-MCM-41 compared to other systems.

The remaining amount of L-Arginine present into porous solid was found to be 19.8% for L-arg_1/Np-MCM-41 and L-arg_2/Np-MCM-41 respectively while 11.7 % in case of L-arg_3/Np-MCM-41. This study shows the complete mass balance.

Kinetics and mechanism

First order release Kinetic Model

In order to understand the release kinetics of L-Arginine, the drug release data of all systems were fitted with first order release kinetics model. Figure 7 shows the first order release kinetic model of L-Arginine release from Np-MCM-41 loaded in different amount. The log percentage remaining was plotted against the time in hour.

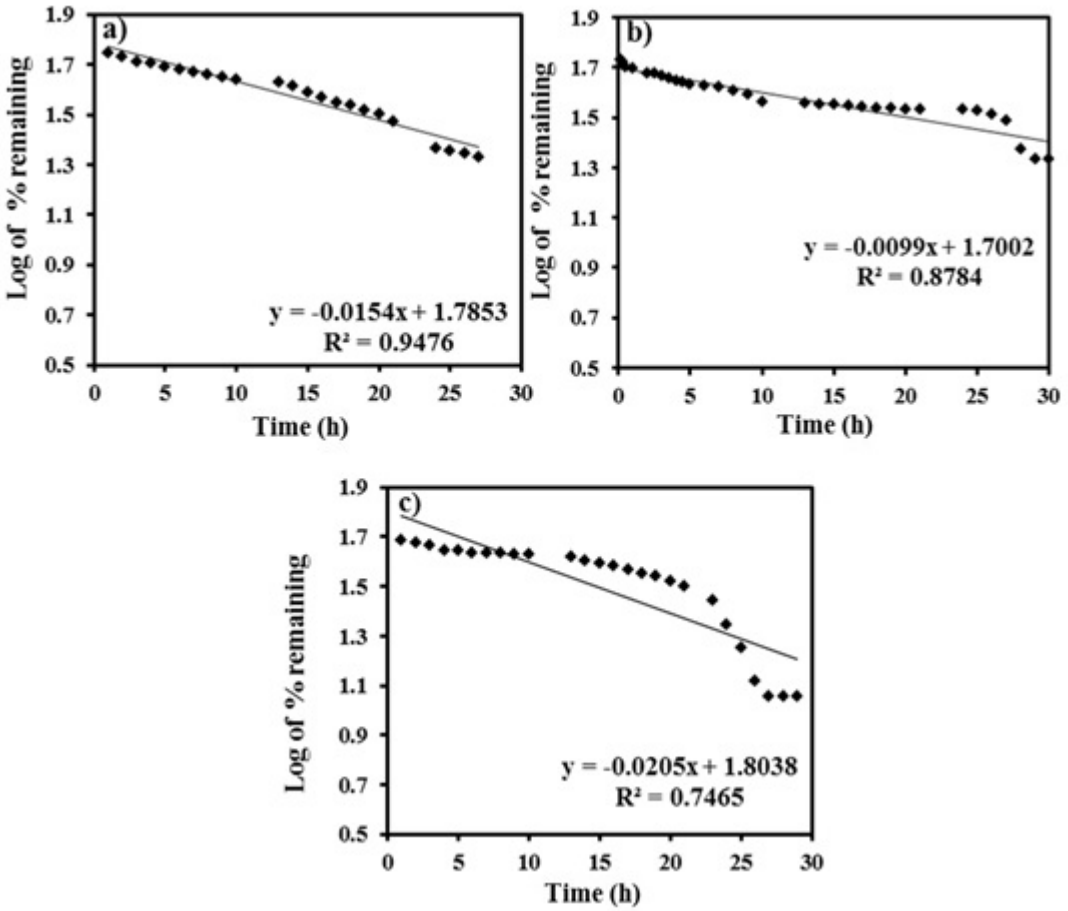

Figure 7. First order release kinetic model of a) L-arg$_1$/Np-MCM-41, b) L-arg$_2$/Np-MCM-41 and (c) L-arg$_3$/Np-MCM-41 (space missing)

The release of L-Arginine follows the first order kinetic with higher linearity and higher correlation coefficient (R^2) value for L-arg$_1$/Np-MCM-41(0.947) compared to L-arg$_2$/Np-MCM-41(0.878) and L-arg$_3$/Np-MCM-41(0.746). The release data for L-arg$_1$/Np-MCM-41 sample was best fitted with first ordered release kinetic model (Figure 7).

Higuchi model

The Higuchi mechanism describes the percentage of release versus square root of time dependent process based on Fickian diffusion. Figure 8 presents the Higuchi model of in vitro release of L-Arginine from Np-MCM-41.The release data for all the system was fitted with Higuchi model for finding the release mechanism.

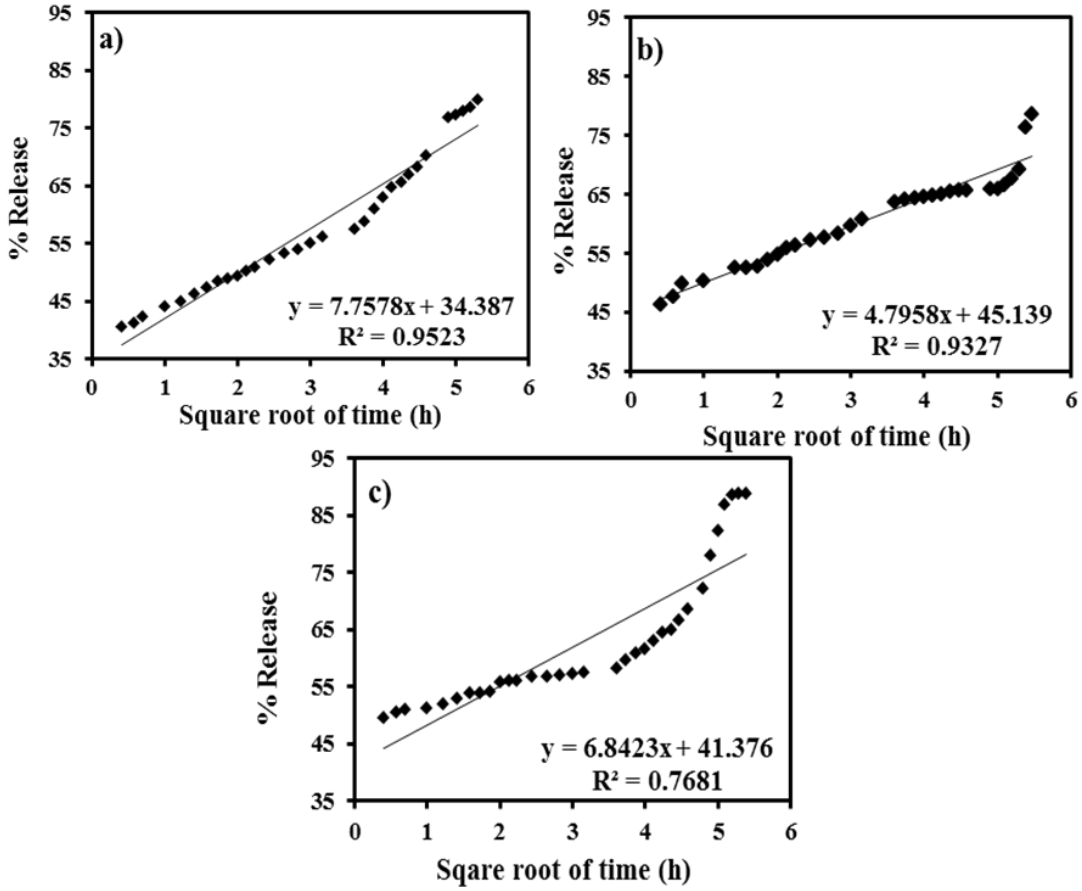

Figure 8. Higuchi model for L-arg$_1$/Np-MCM-41, b) L-arg$_2$/Np-MCM-41 and c) L-arg$_3$/Np-MCM-41

The percentages release data were plotted against the square root of time in h where linear curve is obtained. The release of L-Arginine follows the Higuchi model with higher linearity and higher correlation coefficient (R^2) value for L-arg$_1$/Np-MCM-41 (0.952) compared to L-arg$_2$/Np-MCM-41(0.932) and L-arg$_3$/Np-MCM-41 (0.768) (Figure 8).

The above, in vitro release and kinetic study shows that L-arg$_1$/Np-MCM-41 (100 mg/1 g of Np-MCM-41) is best among all systems. Therefore, this system is further selected for investigating effect of temperature on release rate.

Effect of temperature on release rate

In order to see the effect of temperature, release study from L-arg$_1$/Np-MCM-41 was carried out at body temperature (37 ^oC) and results are shown in Figure 9A. Initially 40% (Figure 9A (a)) and 39% (Figure 9A (b)) of L-Arginine was release at room temperature and body temperature and reached to 55% and 53% up to 10 h. After that slow and controlled release was observed this was reached up to 80% in 28 h for both the systems. Hence there was no significant difference between release profiles in both cases.

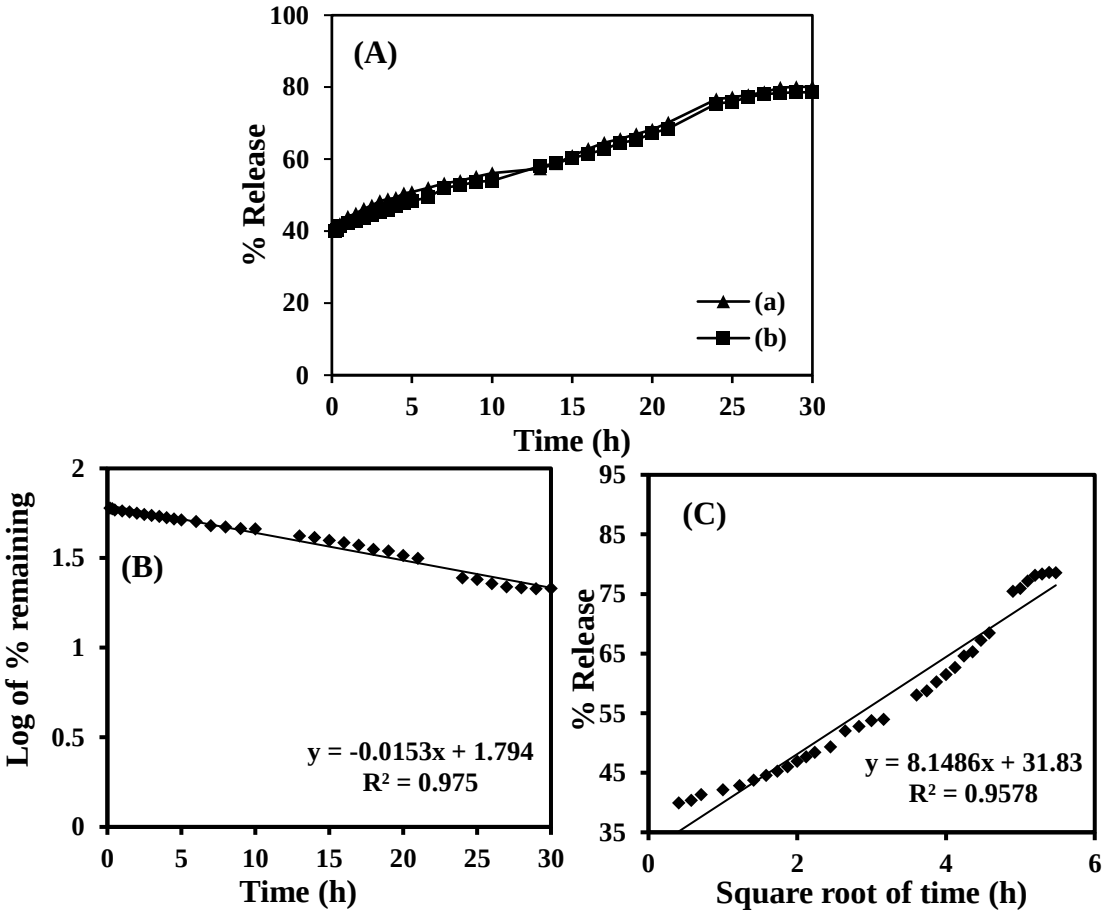

Figure 9. (A) In vitro release profile of L-arg$_1$/Np-MCM-41 **a** at room temperature and **b** at body temperature; (B) First order release kinetic model of L-arg$_1$/Np-MCM-41 and (C) Higuchi model of L-arg$_1$/Np-MCM-41

Further the obtained release data were fitted with first order release kinetic model and Higuchi (Figure 9b and Figure 9c). The release of L-arg$_1$/Np-MCM-41 at body temperature also follows the first order kinetic and Higuchi model. Higher linearity and higher correlation coefficient was observed for release profile at body

temperature compared to release profile determined at room temperature as shown in table 2.

Table 2: L-Arginine release kinetic and mechanism data

Release profile	(Correlation coefficient, R^2)	
	First order release kinetic model	Higuchi Model
At room temperature	0.947	0.952
At body temperature	0.975	0.957

In vitro controlled release of L-Arginine from TPA-Np-MCM-41

Experimental

Materials

12-tungstophosphoric acid was received from Merck of A.R. Grade and used without any further purification.

Functionalization of Np-MCM-41 using TPA

Functionalisation was carried out by incipient wet impregnation method. 30 % of TPA anchored to Np-MCM-41 was synthesized. 1 g of Np-MCM-41 was impregnated with an aqueous solution of TPA (0.3/30 g/mL of distilled water) and dried at 100 ^{o}C for 10 h. The obtained material was designated as TPA-Np-MCM-41.

Synthesis of L-Arginine loaded TPA-Np-MCM-41 (L-arg/TPA-Np-MCM-41)

Series of materials containing 5–15 % of L-Arginine loaded on TPA-Np-MCM-41 were also synthesized by incipient wet impregnation method. TPA-Np-MCM-41 mass of 1 g was impregnated with an aqueous solution of L-Arginine (0.05/5–0.15/15 g mL^{-1}) and pH of the mixture was adjusted up to 4 using 0.1 M HCl solution. Then mixture was dried at 100 ^{o}C for 5 h. The obtained material was designated as L-$arg_{0.5}$/TPA-Np-MCM-41, L-arg_{1}/TPA-Np-MCM-41 and L-$arg_{1.5}$/TPA-Np-MCM-41.

Release study of L-Arginine from TPA-Np-MCM-41

The in vitro L-Arginine release profile was obtained by soaking 0.5 g of L-arg_{1}/TPA-Np-MCM-41 in 62.5 mL of SBF (0.8 mg of L-Arginine in 1 mL SBF) at room temperature and at 200 rpm. At predetermined time interval released fluid was taken (0.5 mL) and immediately equal amount of fresh SBF was added to maintain the constant volume. This release fluid was analyzed for L-Arginine content by treating it with 10 % ninhydrin solution at 570 nm using (systronic) UV–Visible spectrophotometer. Same study was also carried at 37 ^{o}C temp. All the experiments were repeated three times. Further release study was carried out in gastric fluid (GF) at room temperature and under stirring condition.

Results and discussion

Characterizations

EDS analysis for TPA-MCM-41 and L-arg$_1$/TPA-MCM-41 are shown in Table 1. The results obtained from EDS were in good agreement with the theoretical values.

Table 1 Results of elemental analysis in wt%.

Materials	Elemental analysis (weight %)			
	W		P	
	Theoretical	By EDS	Theoretical	By EDS
TPA-Np-MCM-41	19.0	18.0	0.32	0.30
L-arg$_1$/TPA-NpMCM-41	13.5	12.9	0.10	0.09

TGA

TGA of pure TPA, Np-MCM-41, TPA-Np-MCM-41 and L-arg$_1$/TPA-Np-MCM-41 is shown in Figure 10. TPA exhibits weight loss in three stages at 100, 200 and 485 ^{o}C. These can be attributed to initial weight due to adsorbed water, second weight loss due to loss of water of crystallization near 200 ^{o}C to give the Keggin structure, which is stable on heating up to 350 ^{o}C. The weight loss at 485 ^{o}C may be attributed to the decomposition of the Keggin structure of TPA into the simple oxides [6].

TGA of Np-MCM-41 shows initial weight loss of 6.14 % at 100 ^{o}C. This may be due to the loss of adsorbed water molecules. The final 7.92 % weight loss above 450 ^{o}C may be due to the condensation of silanol groups to form siloxane bonds. After that absence of any weight loss indicates that Np-MCM-41 is stable up to 600 ^{o}C. The TGA of TPA-Np-MCM-41 (Figure 1c) shows initial weight loss of 3.6 % due to the loss of adsorbed water. Second weight loss of 1.2 % between 150 and 250 ^{o}C corresponds to the loss of water of crystallization of Keggin ion. Further a gradual weight loss was also observed from 250 to 500 ^{o}C due to the difficulty in removal of water contained in TPA molecules inside the channels of MCM-41 [7]. This type of inclusion causes the stabilization of TPA molecules inside the channels of Np-MCM-41.

TGA of L-arg$_1$/TPA-Np-MCM-41 shows initial weight loss of 1.76 % due to the loss of adsorbed water. Further weight loss of 10.77 %, from 200 to 450 ^{o}C

indicates the removal L-Arginine which also confirms the 10 % loading of Larginine on TPA-Np-MCM-41 (0.1 g L-Arginine per g of Np-MCM-41).

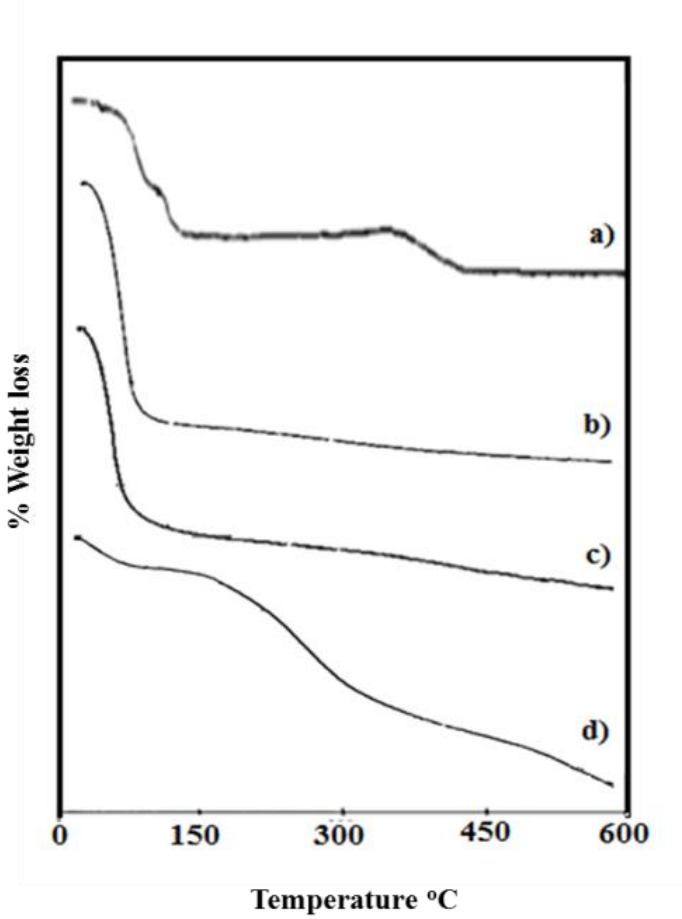

Figure 10. TGA curve of a) TPA, b) Np-MCM-41, c) TPA-Np-MCM-41 and d) L-arg$_1$/TPA-Np-MCM-41

Nitrogen adsorption-desorption isotherm

The nitrogen adsorption–desorption isotherm and pore size distribution curve of the (a) Np-MCM-41, (b) TPA-Np-MCM-41 and (c) L-arg$_1$/TPA-Np-MCM-41 are displayed in Figure 11 and the pore texture are summarized in Table 3. The Nitrogen adsorption desorption isotherm of all three materials are of type IV in nature according to the IUPAC classification and exhibited an H1 hysteresis loop which is a characteristic of mesoporous solids (Figure 11a). The adsorption branch of each isotherm showed as sharp inflection, which means a typical capillary condensation within uniform pores.

The isotherms of TPA-Np-MCM-41 show a comparable and marked decrease in the nitrogen adsorbed volume and hence specific surface area and pore volume are decrease compare to Np-MCM-41, which indicates the partial filling of the mesopores by the TPA moiety bound on the silica pore surface. Decrease in all structural

parameters of TPA-Np-MCM-41 suggests the strong interaction between the TPA moiety and Np-MCM-41 as well as the functionalisation of Np-MCM-41 by TPA moiety did not alter the structure of Np-MCM-41.

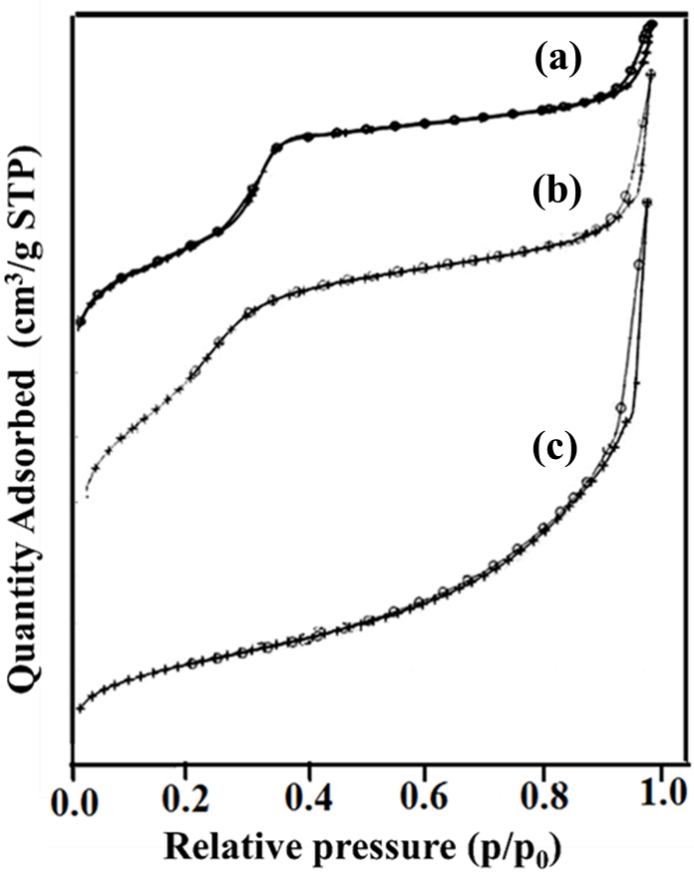

Figure 11. Nitrogen adsorption-desorption isotherm of (a) Np-MCM-41, (b) TPA-Np-MCM-41 and (c) L-arg$_1$/TPA-Np-MCM-41

The isotherm of L-arg$_1$/TPA-Np-MCM-41 show type (IV) pattern with three stages: monolayer adsorption of nitrogen on the walls of mesopores, the part characterized by a steep increase in adsorption due to capillary condensation in mesopores with hysteresis, and multi-layered adsorption on the outer surface of the particle. The drastic decrease in the value of surface area and pore volume also indicate presence of L-Arginine into the mesopores.

Table 3. Textural property of Np-MCM-41, TPA-Np-MCM-41 and L-arg$_1$/TPA-Np-MCM-41

Materials	Specific surface area (m^2/g)	Pore volume (cm^3)/g
Np-MCM-41	1100	1.06
L-Arg$_1$/Np-MCM-41	478	0.44
TPA/Np-MCM-41	791	0.55
L-Arg$_1$/TPA-Np-MCM-41	153	0.34

FTIR

The Figure 12 shows the FTIR spectra of (a) TPA, (b) Np-MCM-41, (c) TPA-Np-MCM-41 and (d) L-arg$_1$/TPA-Np-MCM-41. The FTIR spectrum of MCM-41 shows broad band around 1100–1300 cm^{-1} corresponds to asymmetric stretching vibration of Si–O–Si. The band at 801 and 498 cm^{-1} corresponds to symmetric stretching and bending vibration of Si–O–Si, respectively. The broad band at 3448 cm^{-1} corresponds to symmetric stretching vibration of Si–OH group.

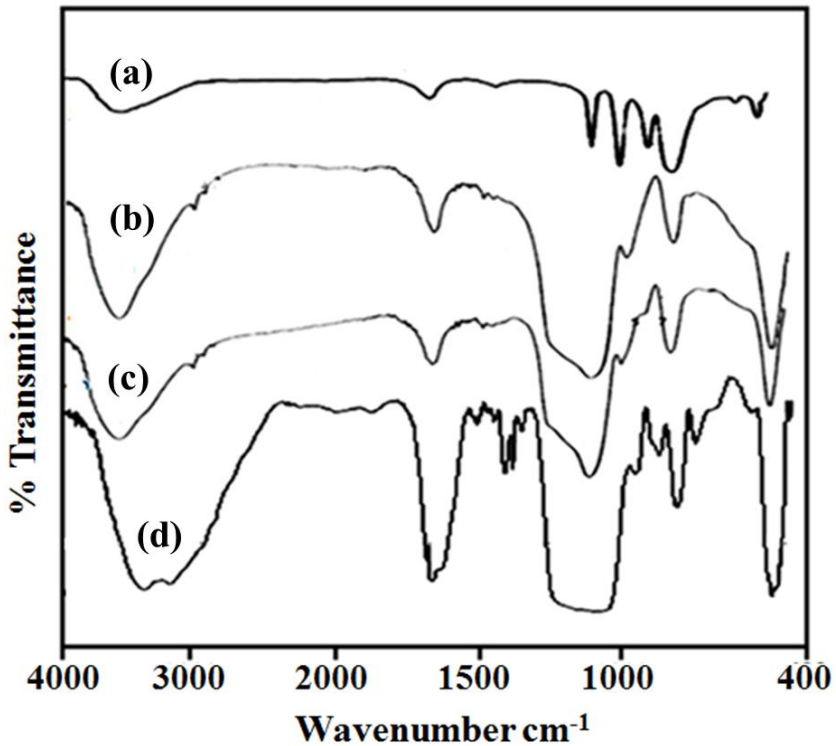

Figure 12. FTIR spectra of a) TPA, b) Np-MCM-41, c) TPA-Np-MCM-41 and d) L-arg$_1$/TPA-Np-MCM-41

FTIR spectrum of TPA-Np-MCM-41 (Figure 12) was almost the same as that of MCM-41. The reported bands for TPA, at 1088, 987, and 800 cm^{-1} corresponding to

W–O–W bending, W–O and P–O symmetric stretching, respectively, were absent in TPA-Np-MCM-41. If TPA is dispersed onto the surface of Np-MCM-41, the mentioned bands for TPA should be seen in the FTIR spectra. The absence of respective FTIR bands of TPA in TPA-Np-MCM-41 may due to the overlapping of TPA bands with that of Np-MCM-41. All the bend of Np-MCM-41 was observed in TPA-Np-MCM-41 which confirms the intact structure of Np-MCM-41.

In addition to strong bands due to the TPA-Np-MCM-41, the FTIR spectrum of L-arg_1/TPA-Np-MCM-41 show vibration band with shifting at 3185, 1696 and 1668 cm-1, and due to N–H stretching vibration and NH_2 in plan bending vibration and C=O stretching vibration. Thus shifting of all bands were observed, however significant shifting in N–H stretching vibration (3151–3185 cm-1) and in C=O stretching vibration (1574–1668 cm-1) confirm the strong interaction mainly hydrogen bonding between the N–H and C=O group of L-Arginine and functionalized TPA moiety of TPA-Np-MCM-41, which was further confirm by 29Si MAS NMR data. So the interaction between the L-Arginine molecule and TPA-Np-MCM-41 mainly depend on orientation of L-Arginine molecule into the TPA-Np-MCM-41. Furthermore, the principle vibration band of the TPA-Np-MCM-41 do not change after the encapsulation of L-Arginine confirm the structure of TPA-Np-MCM-41 remain unchanged.

Low angle Powder XRD

The XRD pattern of TPA, (a) TPA-Np-MCM-41 and (b) L-arg$_1$/TPA-Np-MCM-41 are shown in Figure 13. In the case of TPA-Np-MCM-41, absence of characteristic peaks of crystalline phase of TPA indicates fine dispersion of TPA inside the hexagonal channels of Np-MCM-41. The XRD pattern of L-arg$_1$/TPA-Np-MCM-41 shows slight shifting in the characteristic peak of Np-MCM-41 at 2 Theta = 1.76^o. All most same pattern indicates well dispersion as well as no change in TPA-MCM-41 structure after loading of L-Arginine

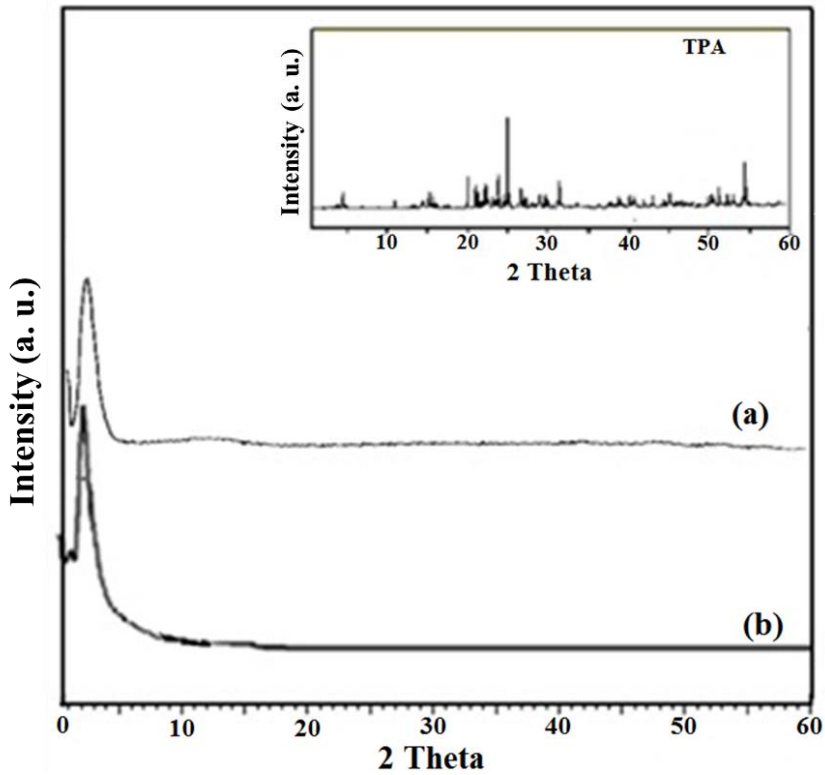

Figure 13. Powder XRD of TPA (inset), a) TPA-Np-MCM-41 and b) L-arg$_1$/TPA-Np-MCM-41

TEM

Figure 14 shows TEM images of Np-MCM-41, TPA-Np-MCM-41 and L-arg$_1$/TPA-Np-MCM-41 at 100 nm. The TEM images of Np-MCM-41 displays the morphology of hexagonal arrays of channels with uniform pore size, at 100 nm resolution. The TEM image of TPA-Np-MCM-41 shows absence of crystalline phase of TPA inside the channels of Np-MCM-41 indicating high dispersion of TPA and absence of agglomeration. The TEM image L-arg$_1$/TPA-Np-MCM-41 also displays almost the same morphology with slight darkening which confirm the multi-layered adsorption of L-Arginine on TPA-Np-MCM-41 agreeing well with BET data. It also suggests that there was no structure degradation of Np-MCM-41.

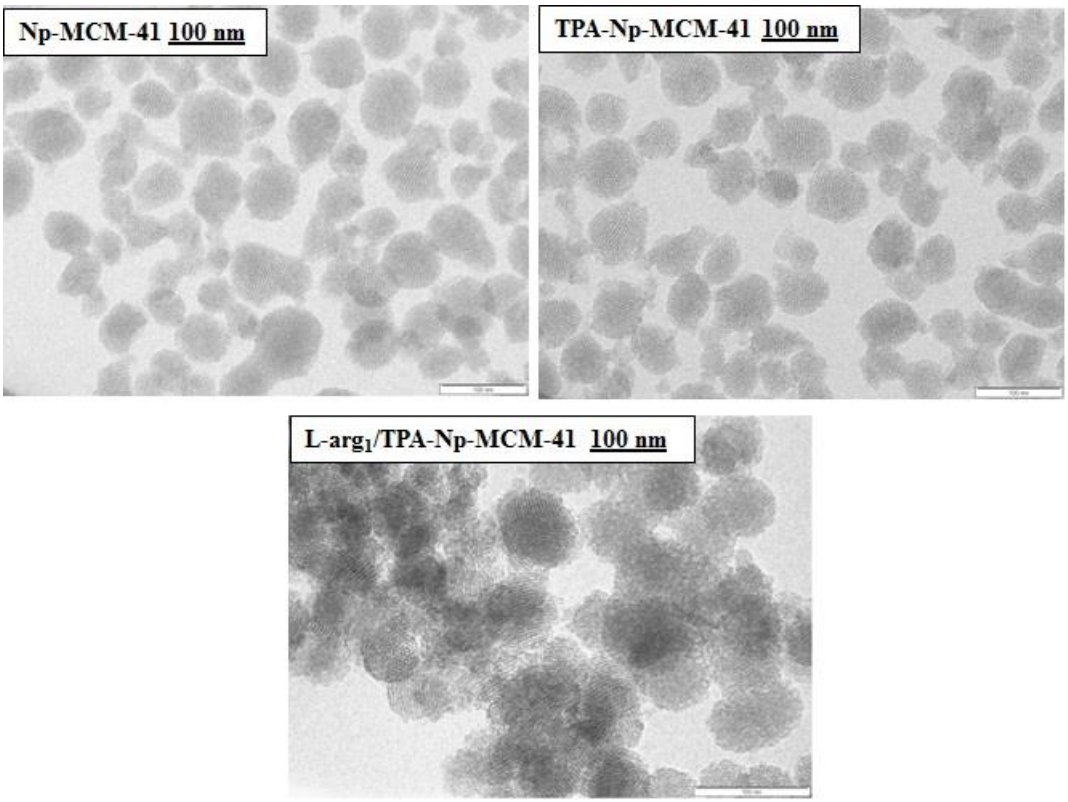

Figure 14. TEM images of pure and L-Arginine loaded materials at 100 nm

In vitro release of L-Arginine from TPA-Np-MCM-41

Effect of stirring on release rate of L-Arginine

L-Arginine release from TPA-Np-MCM-41 was shown in Figure 15a. The release profile shows the existence of two steps: (1) initial burst release and (2) fixed slow release. Initially it show 45 % L-Arginine release and reached to 58 % up to the 10 h and this burst release may be due to the dissolution of L-Arginine molecule adsorbed on the outer surface of TPA-MCM-41. The second step involved fixed slow release rate of L-Arginine molecule. After 10 h slow and more controlled release rate was observed. 64 % L-Arginine was release at 24 h and it reaches up to 80 % after 32 h. So concentration of L-Arginine remains constant for longer period of time in SBF. Over all release profile of L-Arginine shows more controlled and slower release of it.

To see the effect of stirring on the release of L-Arginine, same study was carried out in static condition and release profile was compared with stirring condition (200 rpm) (Figure 15c). In static condition, initially 28 % L-Arginine was released and reached to 43 % within 10 h. After that slow and delayed released was observed and reached to 50 % up to 28 h. The slower release in static condition could be due to the slower diffusion of drug which ultimately decrees the dissolution rate of L-Arginine from TPA-MCM-41 to the bulk, release fluid i.e., SBF and it required high time for complete release of L-Arginine.

Effect of TPA on release rate of L-Arginine

In order to see the role of TPA, L-Arginine release from TPA-Np-MCM-41 was also compared with parent Np-MCM-41 (Figure 15b). Initially 40 and 45 % L-Arginine release from Np-MCM-41 and TPA-Np-MCM-41 and reached up to 56 and 58 % respectively up to the 10 h. After 10 h slow and more controlled release was observed for TPA-Np-MCM-41 compare to parent Np-MCM-41. 76 and 64 % release was observed from Np-MCM-41 and TPA-Np-MCM-41 at 24 h and reached up to 80 % after 28 and 32 h for Np-MCM-41 and TPA-Np-MCM-41, respectively. The in vitro release profile shows that more controlled and delayed release of L-Arginine was observed in case of TPA-Np-MCM-41 compare to parent Np-MCM-41.S The release of L-Arginine from TPA-Np-MCM-41 was also confirmed by FTIR (Figure 16).

It is well known that the pore size [8-10] as well as the interaction of the host guest [11] has a pronounced influence on the kinetics of drug release. Drug delivery rate slows down with the decrease of the pore size. It also decreases with increase in the host–guest interaction i.e. stronger the interaction, slower is the drug delivery rate. In the present case, the slow release of L-Arginine may be due to the following reasons. (1) The strong interaction between L-Arginine molecules with oxygen of TPA was already confirmed by FTIR spectra. (2) It is seen from the Table 2 that the pore volume of L-arg$_1$/TPA-Np-MCM-41 is smaller than the L-Arg$_1$/Np-MCM-41. So there may be restricted diffusion of L-Arginine was occurred from smaller pore volume.

To see the role of TPA, L-arg-TPA salt was synthesized by same procedure which is found to be completely soluble in SBF, distilled water and SGF. This suggests that TPA does not act as carrier but only as a functionalizing agent that holds L-Arginine for longer period of time.

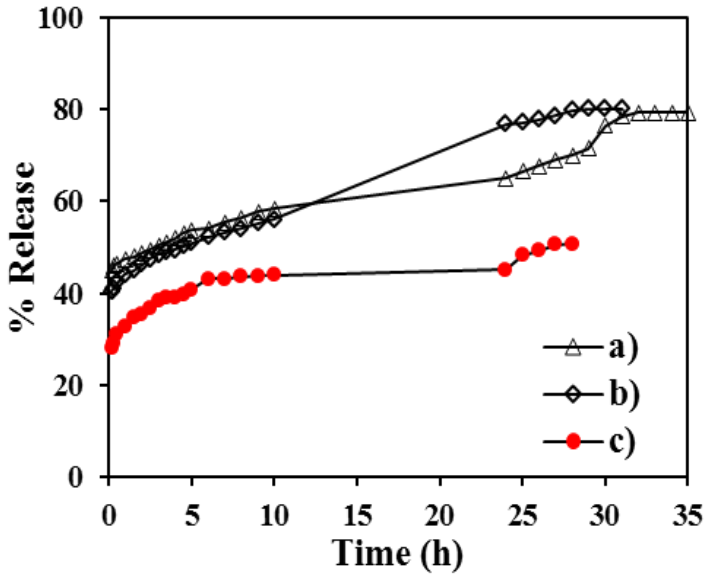

Figure 15. Release profile of a) L-arg$_1$/TPA-Np-MCM-41 (stirring condition), b) L-arg$_1$/Np-MCM-41 and c) L-arg$_1$/TPA-Np-MCM-41 (static condition)

Further, FTIR analysis of L-arg$_1$/TPA-Np-MCM-41 was carried out after release study and spectrum is shown in Figure 16. It is seen from the spectra that the bands correspond to N-H stretching vibration and CH_3 in plan bending vibration are disappeared. This may be due to the removal of L-Arginine from TPA-Np-MCM-41 during the release study. However the bands correspond to NH_2 in plan bending vibration and C=O stretching vibration show slight shifting with lower intensity. This suggests that some amount of L-Arginine was remaining inside the TPA-Np-MCM-41. That was also confirm from release study as it shows that 80% L-Arginine was release up to 32 h and then it became constant.

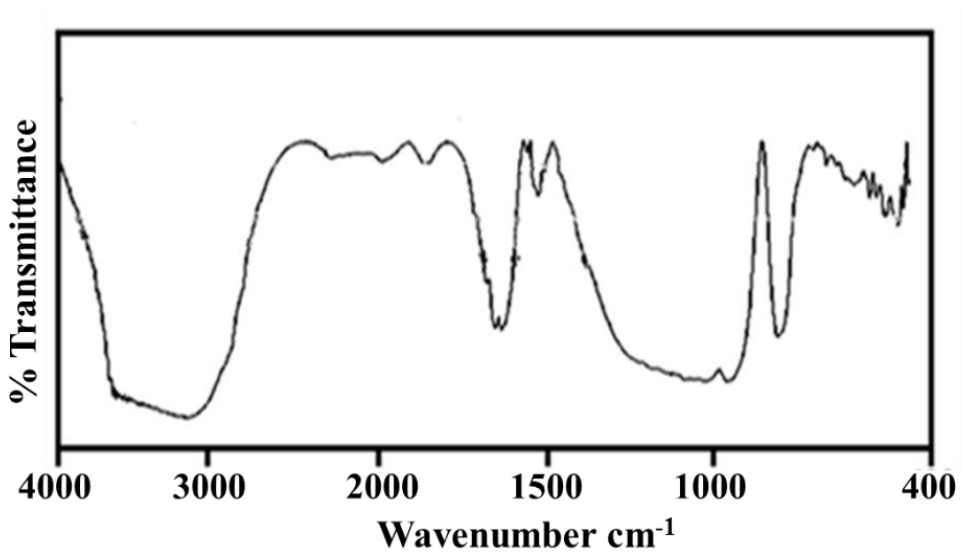

Figure 16. FTIR spectrum of L-arg$_1$/TPA-Np-MCM-41 after release study

Effect of pH and temperature on release of L-Arginine

In order to see the effect of pH on release of L-Arginine, a comparative study was carried out in SBF (pH 7.4) and SGF (pH 1.2) and results are shown in Figure 17A. In acidic pH slow release was observed, as L-Arginine acquire two positive charges and remain as arg^{2+} which may have strong interaction with terminal oxygen of TPA moiety which will slow down the diffusion of L-Arginine molecules. While at pH 7.4, L-Arginine remains as arg^{+} which has comparatively weak interaction which allows the easy diffusion of it**.**

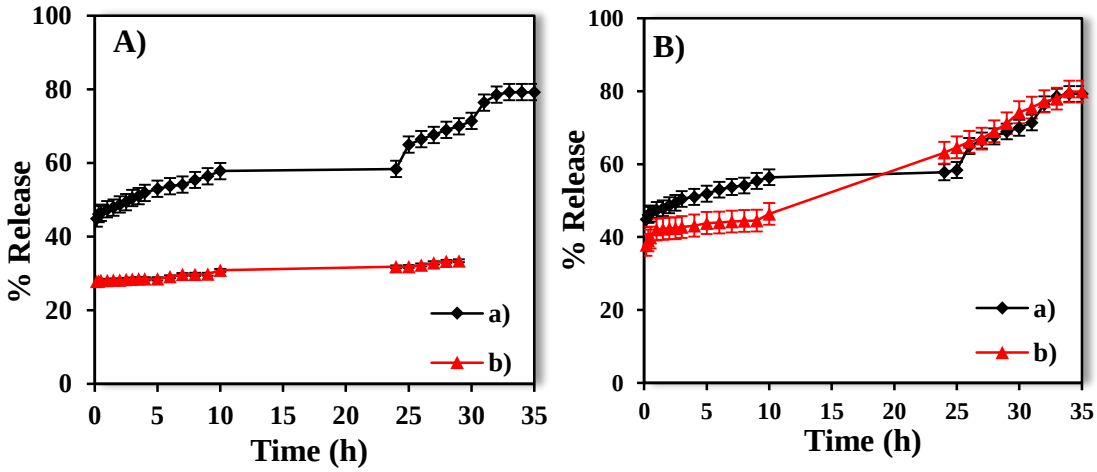

Figure 17. A) Release profile of L-arg_1/TPA-Np-MCM-41 a) in SBF (pH 7.4) and b) in GF (b, pH 2) and **B)** release profile of L-arg_1/TPA-Np-MCM-41 a) at room temperature and b) at 37 ^{o}C temperature

Similarly to see the effect of temperature, the release study was carried out at 37 ^{o}C (body temperature) as well as at room temp (Figure 17B). Initially 5–10 % difference was observed up to 10 h. However, a slow release profile was observed after 10 h for both the condition. There was no significant difference between the release profiles of these two systems and the results were comparable.

Effect of loading amount on release profile of L-Arginine

To see the effect of loading on release profile, different amount of L-Arginine loaded TPA-MCM-41 were synthesized and release profile was compared. From the Figure 18, it is clear that as the amount of L-Arginine increases, release rate increase. Initially burst release was observed which may be due to the presence of large amount of L-Arginine molecules on the outer surface of TPA-Np-MCM-41. However, slow release

was observed after 10 h for all the three systems. Further as the amount of drug increase, the possibility of blocking of channels and pores increase which affect the mesoporous structure of Np-MCM-41.

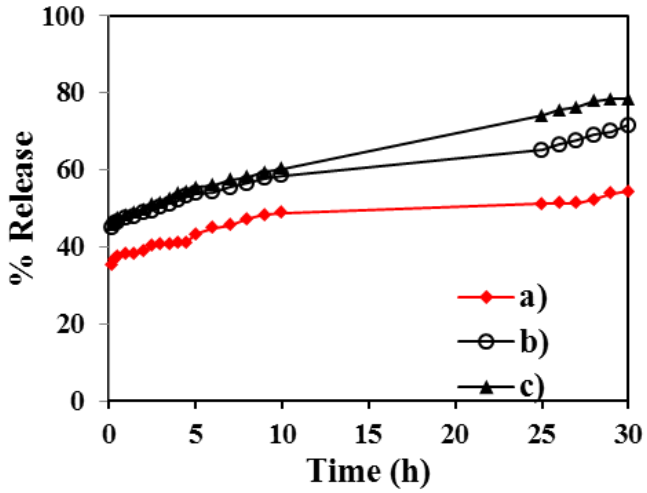

Figure 18. Release profile of a) L-arg$_{0.5}$/TPA-Np-MCM-41, b) L-arg$_{1}$/TPA-Np-MCM-41 and c) L-arg$_{1.5}$/TPA-Np-MCM-41

Kinetics and mechanism

For finding drug release mechanism and drug release kinetic the in vitro L-Arginine release data was fitted with first order release kinetic model and Higuchi model.

According to First order release kinetic model rate of release is concentration dependent. Figure 19A shows the first order release kinetic model of L-Arginine from TPA-Np-MCM-41 where Log of percentage remaining data was plotted against time. The release of L-Arginine was followed the first order kinetic with linearity and correlation coefficient (R^2) value for TPA-Np-MCM-41 (0.919).

The Higuchi model (Figure 19B) describes the percentage release versus square root of time dependent process based on Fickian diffusion. According to this model release mechanism of L-Arginine involves simultaneous penetration of SBF into the pores, dissolution of drug molecule and diffusion of these molecules from the pores. The in vitro L-Arginine release data was best fitted with Higuchi model. The release mechanism of L-Arginine was best explained by this model with high linearity and high correlation coefficient (R^2) value (0.940).

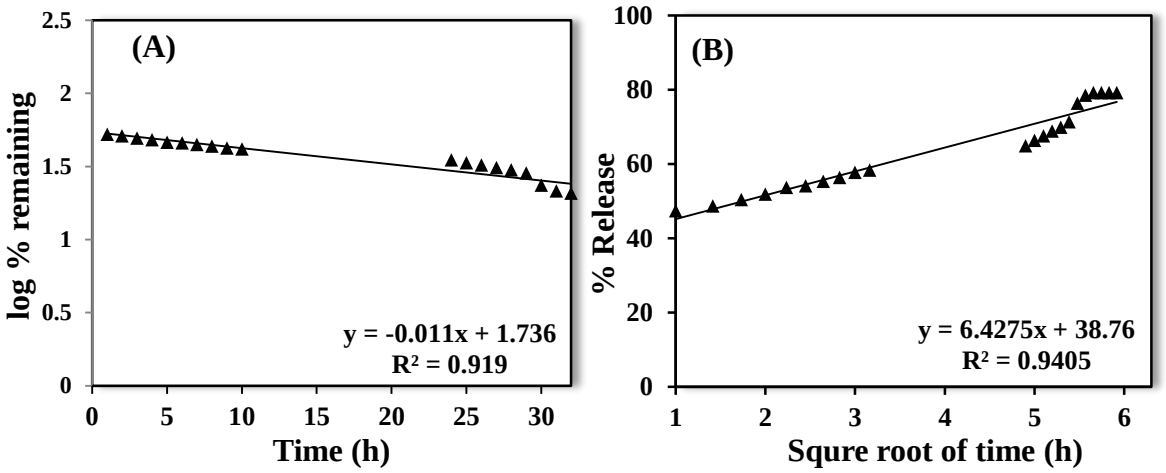

Figure 19. (A) First order release kinetic model and (B) Higuchi model of L-Arginine from TPA-Np-MCM-41

Thus, L-Arginine release from TPA-Np-MCM-41 is concentration dependent process and follows First order release kinetics. Further it follows the Fickian diffusion mechanism.

Part B

In vitro release study of Aspirin and Captopril from Np-MCM-41 and TPA-Np-MCM-41

Experimental

Loading of Aspirin and Captopril into Np-MCM-41 and TPA-Np-MCM-41

Loading of Aspirin and Captopril was carried out by same method as stated in chapter 2. Aspirin loaded into Np-MCM-41 and TPA-Np-MCM-41 were designated as Asp/Np-MCM-41 and Asp/TPA-Np-MCM-41. Captopril loaded into Np-MCM-41 and TPA-Np-MCM-41 was denoted as Cap/Np-MCM-41 and Cap/TPA-Np-MCM-41. The amount of drug loading was obtained by analyzing filtrate using UV-Visible spectrophotometer at 296 nm and 203 nm for Aspirin and Captopril respectively.

In vitro release study of Aspirin/Captopril

In vitro release of Aspirin and Captopril was obtained by same method as stated in chapter 3 and 6. Drug loaded materials (Asp/Np-MCM-41 and Asp/TPA-Np-MCM-41) were soaked in 100 mL of SBF at 200 rpm at 37 ^{o}C temperature under stirring as well as static condition. At proper time interval, 1 mL of release fluid was taken and fresh SBF was added to maintain the constant volume of the system. The 1 mL fraction was diluted and analyzed for drug content using UV-Visible spectrophotometer. Same release study was also carried out in simulated gastric fluid (pH 1.2) to see the effect of pH on release rate. For finding, whether drug molecules are present only on the surface or in the channels of nanoparticles, release study of physical mixture of drug and carrier were also carried out using same method as stated earlier.

Results and Discussion

Characterizations

The drug loading amount was obtained by two methods: (1) By UV-Visible spectroscopic analysis, which is by analyzing the obtained filtrate after loading. (2) By TGA analysis of drug loaded materials. The values obtained by both the methods are presented in Table 1 which is in good agreement with each other. Lower amount of drug loading is observed in case of TPA-Np-MCM-41 as compared to pure Np-MCM-41. This is because; mesoporous channels of MCM-41 are already filled with TPA. So there is lesser space for accommodation of drug molecules.

TGA

Figure 1 shows TGA analysis of all the materials. TGA of Np-MCM-41 shows initial weight loss of 2.7 % at 100 ^{o}C. This may be due to the loss of adsorbed water molecules. The final 4.83 % weight loss above 300 ^{o}C may be due to the condensation of silanol groups to form siloxane bonds. TGA curves of Asp-Np-MCM-41 and Cap/Np-MCM-41 shows initial weight loss of 3.2% and 1.2% up to 150 ^{o}C due to the adsorbed water. Further weight loss of 5.8% and 6.7% from 200 ^{o}C to 550 ^{o}C is may be due to the removal of drugs from Np-MCM-41, respectively.

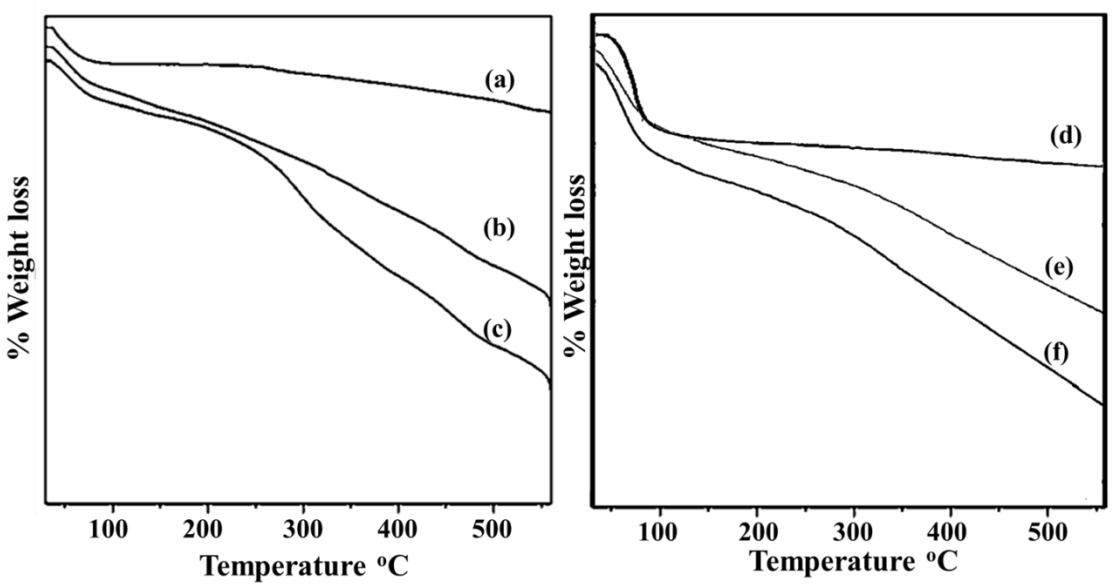

Figure 1. TGA curve of (a) Np-MCM-41, (b) Asp/Np-MCM-41, (c) Cap/Np-MCM-41, (d) TPA-Np-MCM-41, (e) Asp/TPA-Np-MCM-41 and (f) Cap/TPA-Np-MCM-41

TGA of TPA-Np-MCM-41 (Figure 1) shows initial weight loss of 3.8 % due to the loss of adsorbed water. Second weight loss of 1.2% between 150 and 250 ^{o}C corresponds to the loss of water of crystallization of Keggin ion. Further a gradual weight loss was also observed from 250 to 500 ^{o}C due to the difficulty in removal of water contained in TPA molecules inside the channels of MCM-41. TGA curves of Asp/TPA-Np-MCM-41 and Cap/TPA-Np-MCM-41 shows initial weight loss of 2.4% and 3.2% up to 150 ^{o}C due to the adsorbed water. Further weight loss of 3.9% and 4.8% from 200 ^{o}C to 550 ^{o}C is may be due to the removal of drugs from Np-MCM-41, respectively.

Nitrogen adsorption-desorption isotherm

Nitrogen adsorption desorption isotherm of all materials are shown in Figure 2 and textural parameter are shown in Table 1. Isotherm of Np-MCM-41 is type IV in nature suggesting mesoporous structure of Np-MCM-41. Drug loaded materials (Asp/Np-MCM-41 and Cap/Np-MCM-41) and TPA-Np-MCM-41 also shows similar pattern of isotherm. Decrease in surface area and pore volume in drug loaded Np-MCM-41 suggests the insertion of Aspirin and Captopril into the porous channel. A similar result was also observed for TPA-Np-MCM-41 which suggests the functionalization of Np-MCM-41. Isotherm of Asp/TPA-Np-MCM-41 and Cap/TPA-Np-MCM-41 shows deviation from type IV, due to the multilayered adsorption of drugs. Further, significant decrease in surface area and pore volume, in case of Asp/TPA-Np-MCM-41 and Cap/TPA-Np-MCM-41 as compared to TPA-Np-MCM-41, is because of further loading of drug into TPA-Np-MCM-41. As Np-MCM-41 is already filled with TPA and hence there is lesser space for accommodation of drug.

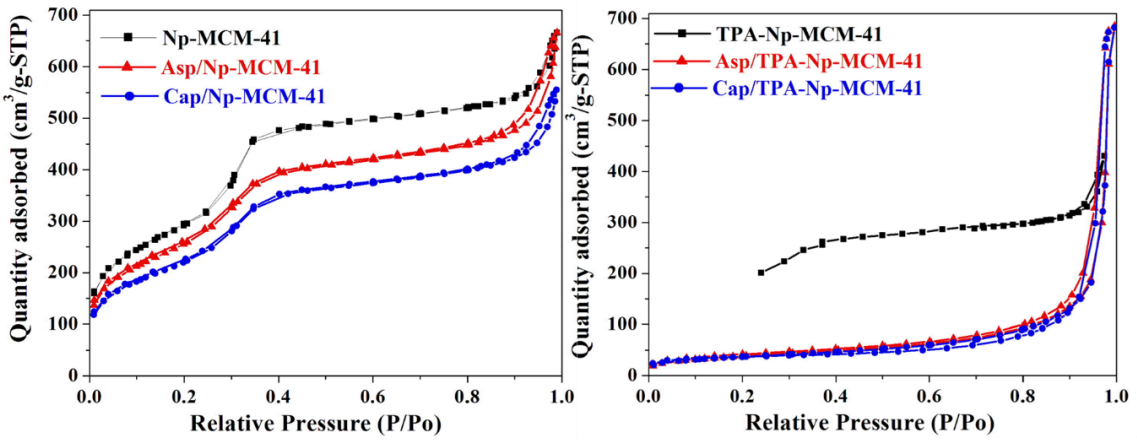

Figure 2. Nitrogen adsorption-desorption isotherm of all materials

Table 1 Textural property of drug loaded and pure materials

Materials	Specific surface area (m^2/g)	Pore volume (cm^3/g)	Amount of drug loaded (mg/g of material)
Np-MCM-41	1100.0	1.06	-
Asp-Np-MCM-41	976	0.44	58±2
Cap-Np-MCM-41	839	0.87	67±2
TPA-Np-MCM-41	791	0.55	-
Asp/TPA-Np-MCM-41	136	0.32	39±2
Cap/TPA-Np-MCM-41	129	0.30	48±2

FTIR

Figure 3 shows FTIR spectra of Np-MCM-41, Cap-Np-MCM-41, Asp-Np-MCM-41, TPA-Np-MCM-41, Asp/TPA-Np-MCM-41 and Cap/TPA-Np-MCM-41. The FTIR spectrum of Np-MCM-41 shows broad band around 1100–1300 cm^{-1} corresponds to asymmetric stretching vibration of Si–O–Si (Figure 3a). The band at 801 and 498 cm^{-1} corresponds to symmetric stretching and bending vibration of Si–O–Si, respectively. The broad band at 3448 cm^{-1} corresponds to symmetric stretching vibration of Si–OH group

Entire bands related to Np-MCM-41 are present in Cap-Np-MCM-41 (Figure 3b). Along with this shifting in band of SH and C=O groups are observed from 2567 cm^{-1} to 2365 cm^{-1} and 1747 cm^{-1} to 1638 cm^{-1} respectively. This suggests the interaction of SH and C=O group of Captopril with Np-MCM-41.

The FTIR spectrum of Asp-Np-MCM-41 shows all bands correspond to Np-MCM-41. Bands corresponds to Aspirin were absent in Asp-Np-MCM-41. a strong band at 1638 cm^{-1} and 966 cm^{-1} are observed correspond to C=O stretching vibration and C-O stretching vibration. Shift in this band from 1630 to 1638 cm^{-1} as well as from 1020 cm^{-1} to 966 cm^{-1} suggests the interaction of carbonyl group of Aspirin with Si-OH group of Np-MCM-41.

The reported bands for TPA, at 1088 and 987 corresponding to P–O symmetric stretching, W–O–W bending respectively, are absent in TPA-Np-MCM-41 (Figure 3d). The absence of respective FTIR bands of TPA in TPA-Np-MCM-41 may due to the overlapping of TPA bands with that of Np-MCM-41. All the bend of Np-MCM-41 was

observed in TPA-Np-MCM-41 which suggests the intact structure of Np-MCM-41 even after functionalization.

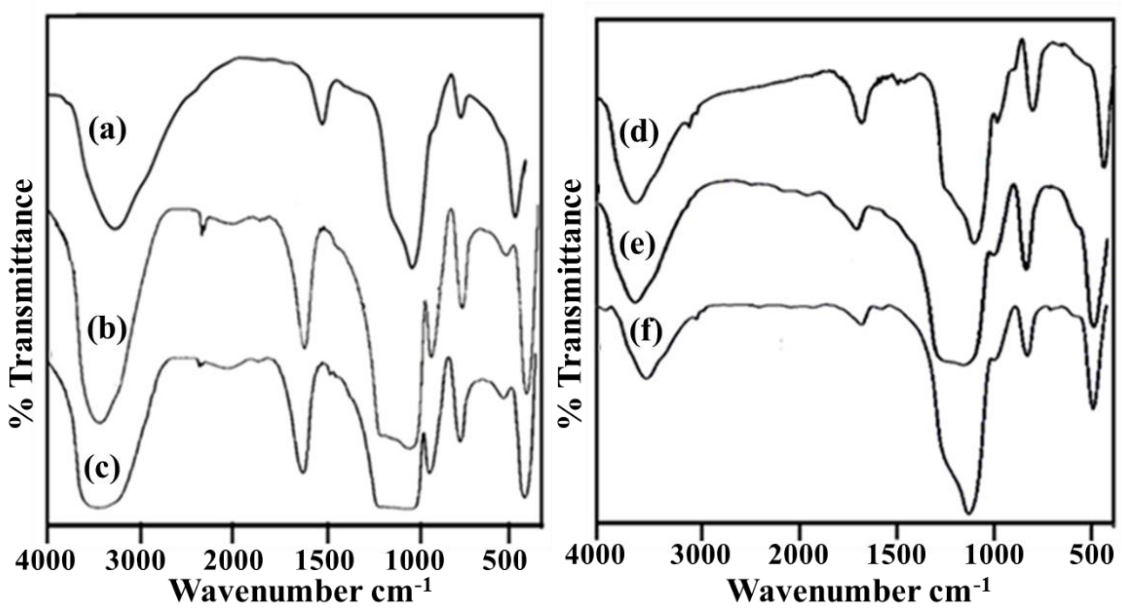

Figure 3. FTIR spectra of (a) Np-MCM-41, (b) Cap/Np-MCM-41, (c) Asp/Np-MCM-41, (d) TPA-Np-MCM-41, (e) Asp/TPA-Np-MCM-41 and (f) Asp/TPA-Np-MCM-41

The FTIR spectra of Asp/TPA-NP-MCM-41 and Cap/TPA-NP-MCM-41 shows similar bands as observed in TPA-Np-MCM-41. However, they shows additional bands at 1627 cm^{-1} and 1635 cm^{-1} corresponding to C=O stretching vibration. Shifting in this bands suggest that drug molecules interact with carrier through this C=O group.

Low angle powder XRD

Figure 4 shows low angle powder XRD of Np-MCM-41, Cap-Np-MCM-41, Asp-Np-MCM-41, TPA-Np-MCM-41, Asp/TPA-Np-MCM-41 and Cap/TPA-Np-MCM-41. The XRD of Np-MCM-41 displays an intense diffraction peak at 2θ = 2.43° which are assigned to the lattice faces (100), suggesting a hexagonal symmetry of Np-MCM-41. The XRD spectra of rest of the materials also shows main characteristic peak at 2θ = 2.43° suggesting intact structure of Np-MCM-41. However, they show decrees in intensity of peak which clearly indicate the insertion of drug into the mesoporous channels of Np-MCM-41.

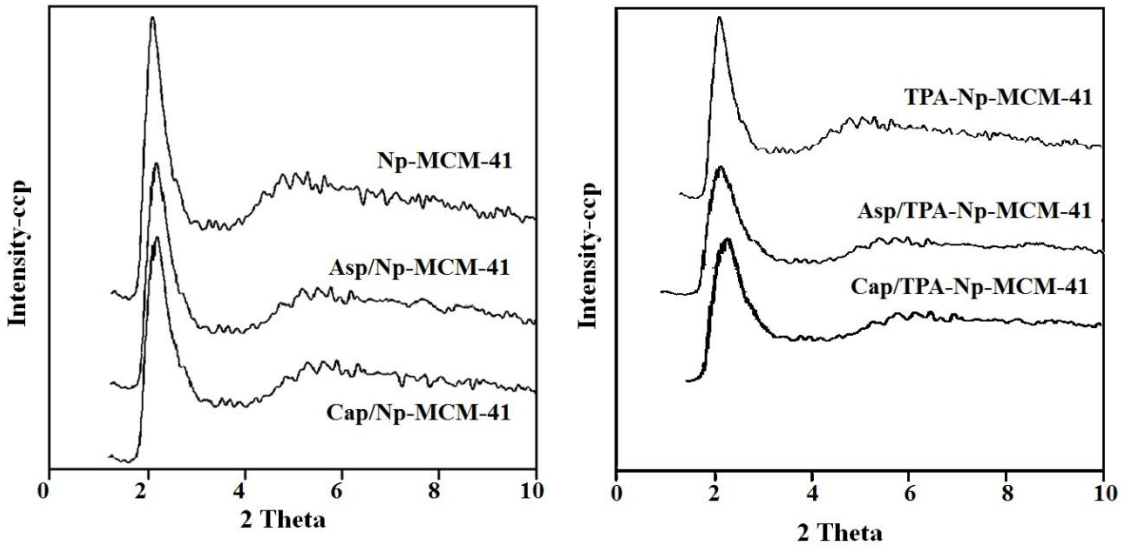

Figure 4. Low angle Powder XRD of pure and drug loaded materials

TEM

TEM images of all the synthesized materials are shown in Figure 5 at 100 nm magnification. TEM images of Np-MCM-41 type MSN shows mono-dispersed nearly spherical morphology with the size of ~52.6 nm. TEM images confirmed the presence hexagonal arrays of channels as well as well-ordered, mono-dispersed porous structure. Comparing the TEM image of drug loaded Np-MCM-41 and pure Np-MCM-41, the dug loaded Np-MCM-41 shows same morphology with uniform distribution of drug into the channels of Np-MCM-41. Further the absence of any agglomeration suggests the well dispersion of drug into it for all the materials.

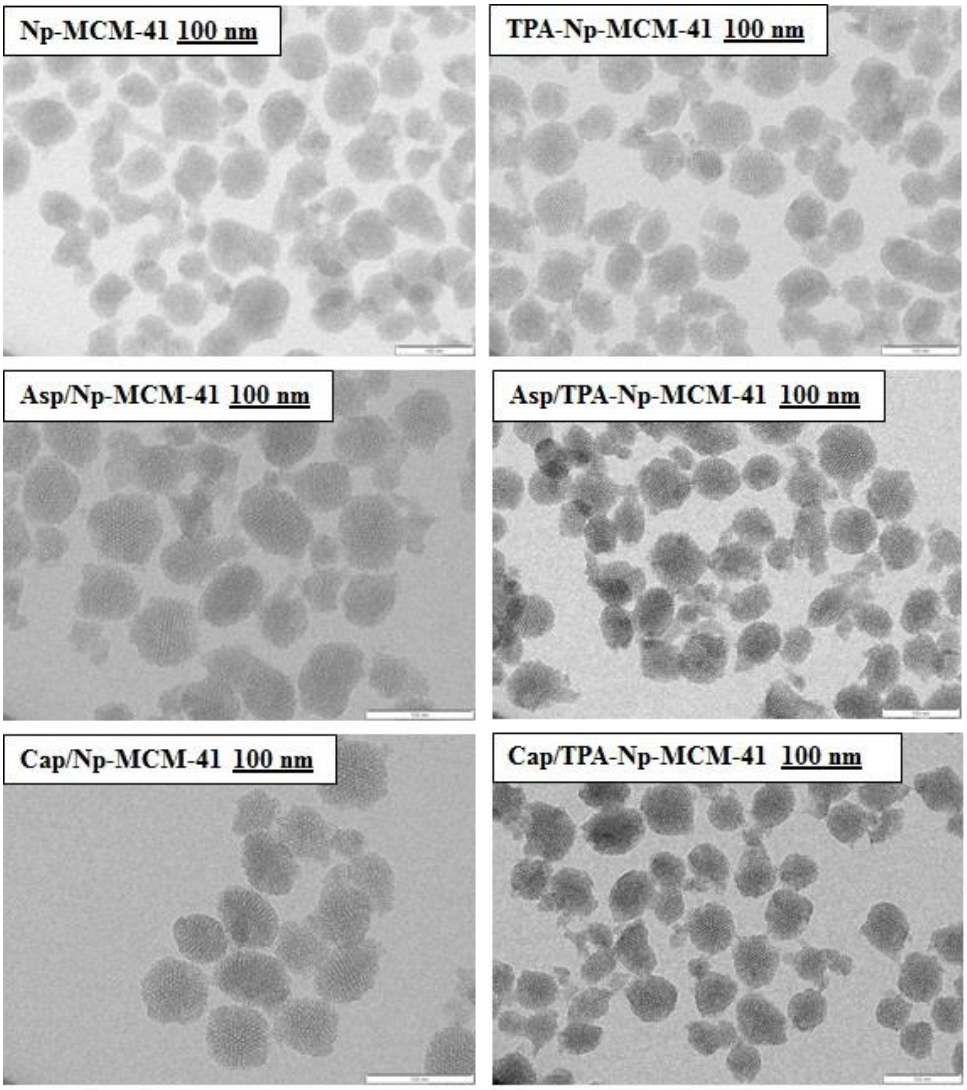

Figure 5. TEM images of Np-MCM-41, TPA-Np-MCM-41, Asp/NP-MCM-41, Asp/TPA-Np-MCM-41, Cap/Np-MCM-41 and Cap/TPA-Np-MCM-41

In vitro release of Aspirin

(i) Comparison with physical mixture

Aspirin loading was carried out by soaking method and hence to see whether the drug molecules only present on the outer surface of material or not, release profile of Aspirin loaded material and physical mixture of Aspirin as well as carrier was compared and shown in Figure 6.

It is clear from the Figure 6 that physical mixture shows 100% dissolution of Aspirin within 1 h. while Aspirin loaded material shows controlled and ordered release which suggests the presence of Aspirin molecule inside the channel of carrier. This is already confirmed by BET surface area analysis.

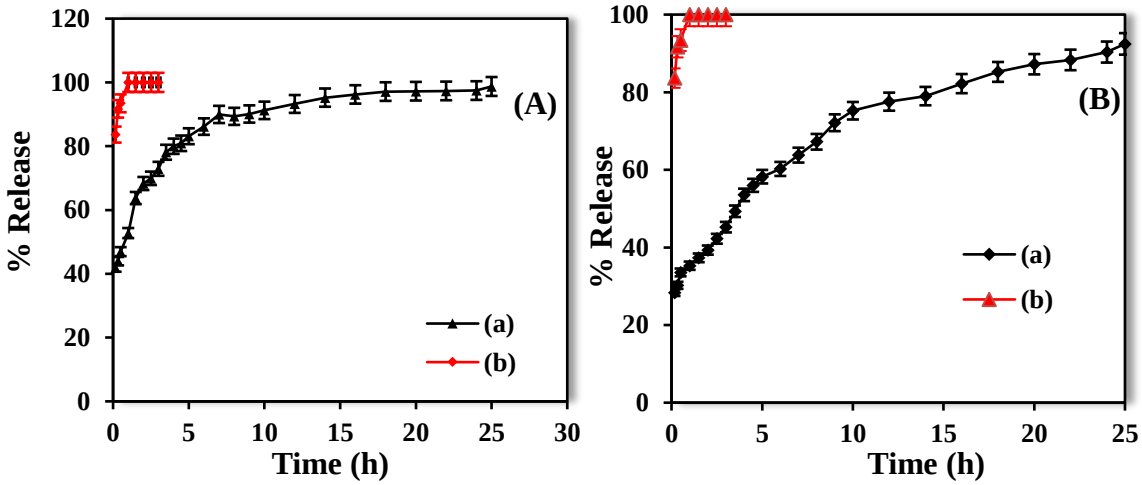

Figure 6. Comparison of release profile of (A) **a** Asp/Np-MCM-41 and (B) **a** Asp/TPA-Np-MCM-41 with **b** physical mixture

(ii) Effect of stirring on release rate of drug

To investigate the effect of stirring on release rate of Aspirin, in vitro release study was carried out in two different conditions: (1) stirring as well as (2) static and results are shown in Figure 7. Under stirring condition, initially 41% Aspirin is released and reached to 98% up to 28 h for Asp/Np-MCM-41 while in case of Asp/TPA-Np-MCM-41; initially 28% of drug is released and reached to 98% up to 25 h. However, under static condition for both systems, slower release was observed which may be due to the slower diffusion of drug (Figure 7).

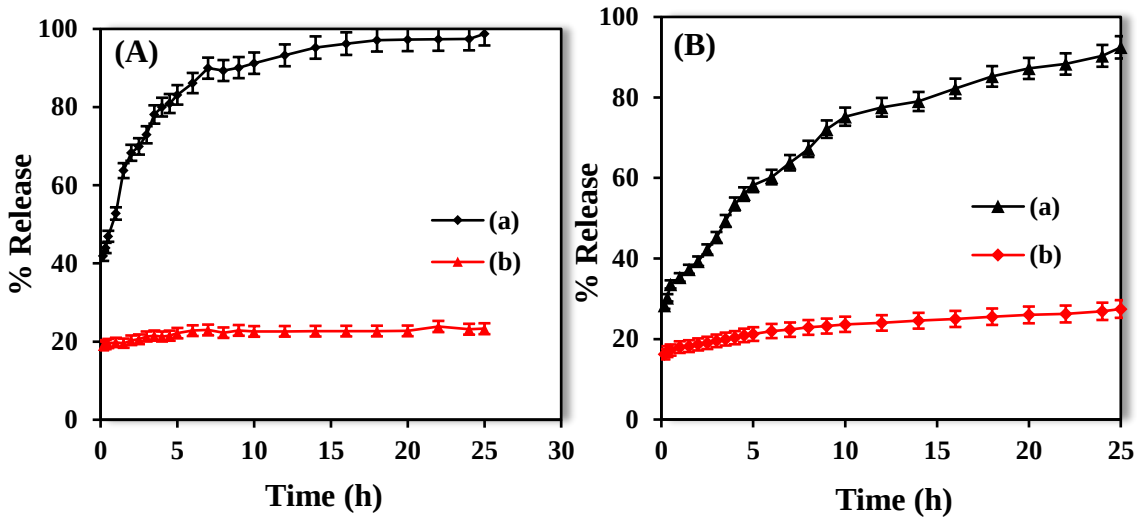

Figure 7. In vitro release profile of (A) Asp/Np-MCM-41 and (B) Asp/TPA-Np-MCM-41 under (a) stirring and (b) static condition

(iii) Effect of pH on release rate of drug

To examine the effect of pH on release rate of drug, release study was also carried out in simulated gastric fluid (SGF, pH 1.2) and compered with release profile obtained in simulated body fluid (SBF, pH 7.4) (Figure 8). For both systems: Asp/NP-MCM-41 and Asp/TPA-Np-MCM-41, faster release of drug is observed at pH 1.2 compared to at pH 7.4. This may be due that protonation of COOH group of Aspirin was occurred at pH 1.2 and hence C=O group is no more present for hydrogen bonding with surface Si-OH group of materials (scheme 1). Thus, the interaction between Aspirin and materials become weak and hence faster release is observed under SGF.

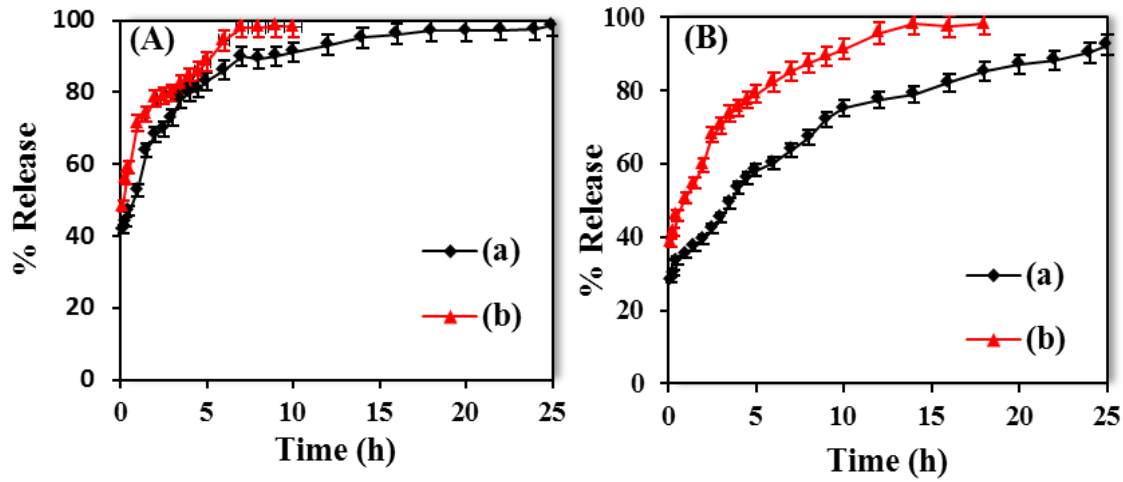

Figure 8. In vitro release profile of (**A**) Asp/Np-MCM-41 and (**B**)Asp/TPA-Np-MCM-41 in (a) SBF (pH 7.4) and (b) SGF (pH 1.2)

In vitro release of Captopril

(i) Comparison with physical mixture

In vitro release profile of Captopril was also compared with physical mixture of drug as well as carrier and results are shown in Figure 9. In this case also physical mixture shows 100% dissolution of Captopril within 1 h. while Captopril loaded material shows controlled and ordered release which suggests the presence of Captopril molecule inside the channel of carrier.

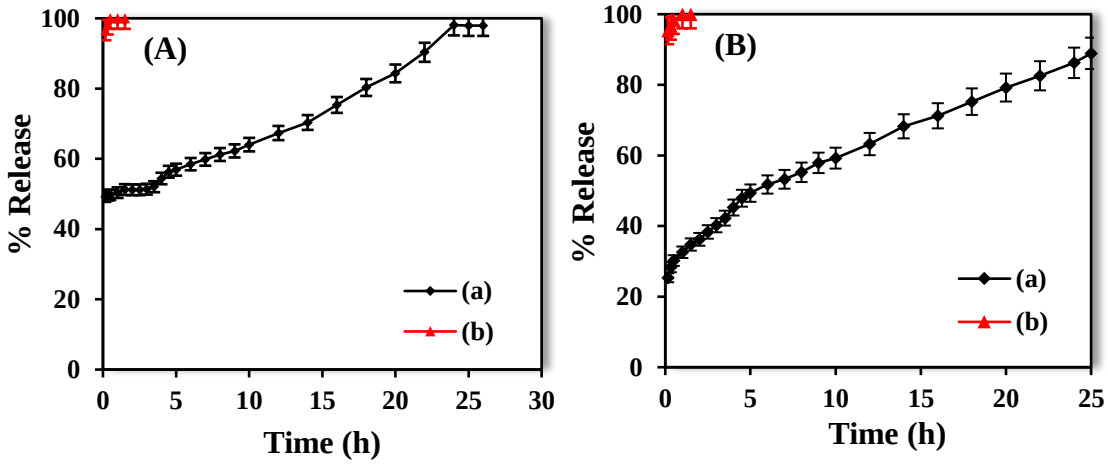

Figure 9. Comparison of release profile of (A) **a** Cap/Np-MCM-41 and (B) **a** Cap/TPA-Np-MCM-41 with **b** physical mixture

(ii) Effect of stirring on release rate of drug

In vitro release study of Cap/Np-MCM-41 and Cap/TPA-Np-MCM-41 were also carried out under stirring as well as static and results are shown in Figure 10. Under stirring condition, initially 49% Captopril is released and reached to 98% up to 26 h for Cap/Np-MCM-41 while in case of Capp/TPA-Np-MCM-41; initially 25% of drug is released and reached to 88% up to 25 h. Here, also under static condition, slower release was observed as in earlier case (Figure 10).

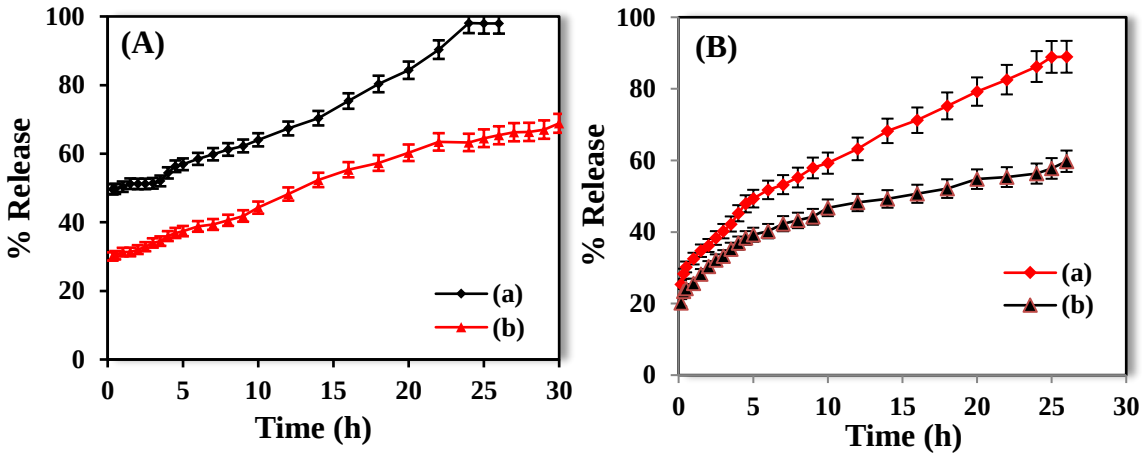

Figure 10. In vitro release profile of (A) Cap/Np-MCM-41 and (B) Cap/TPA-Np-MCM-41 under (a) stirring and (b) static condition

(iii) Effect of pH on release rate of drug

In vitro release profiles of Captopril obtained in different pH (1.2 and 7.4) are also compared and results are shown in Figure 11. At lower pH (SGF), higher release rate was observed compared to high pH (SBF) which is may be because of the action of COOH group of Captopril. However, slower release was obtained for Cap/TPA-Np-MCM-41 compared to Cap/Np-MCM-41. Here also TPA play major role in release rate of drug which was further explained in section (iv).

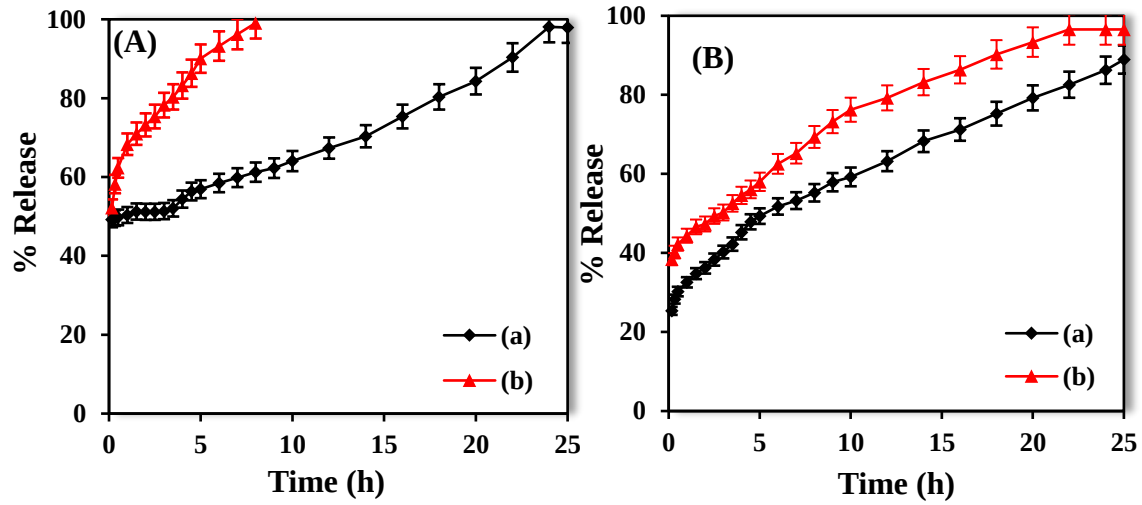

Figure 11. In vitro release profile of (A) Cap/Np-MCM-41 and (B) Cap/TPA-Np-MCM-41 in (a) SBF (pH 7.4) and (b) SGF (pH 1.2)

Effect of TPA on release rate of drugs (Aspirin/Captopril)

To investigate the action of TPA on release rate of drugs, release profile of drug loaded into pure materials were compared with functionalized materials and results are shown in Figure 12. Initially, 41% and 28% of Asp is released and reached to 91% and 75% up to 10 h from MCM-41 and TPA-MCM-41, respectively. It reached to 98% up to 28 h and 25 h for MCM-41 and TPA-MCM-41, respectively. Here, more controlled release profile is obtained from TPA-MCM-41 as compared to pure MCM-41. For Cap, initially, 49% is released and reached to 64% up to 10 h from Np-MCM-41. While in case of Cap/TPA-Np-MCM-41, initially 25% drug is released and reached to 59%. It reached to 98% and 88% up to 25 h for Np-MCM-41 and TPA-Np-MCM-41, respectively.

Burst release is observed for drugs which were loaded into pure Np-MCM-41. This may be due the release of drug molecules which are present on the surface of carrier. However, more controlled release profile is obtained from TPA-Np-MCM-41 as compared to pure Np-MCM-41 for both the drugs. This is may be because of the more interaction between the drug molecules and TPA-Np-MCM-41. As stated earlier, TPA has terminal free oxygen through which it can bind with drug. This may be the reasons of slower release of drugs from TPA-Np-MCM-41.

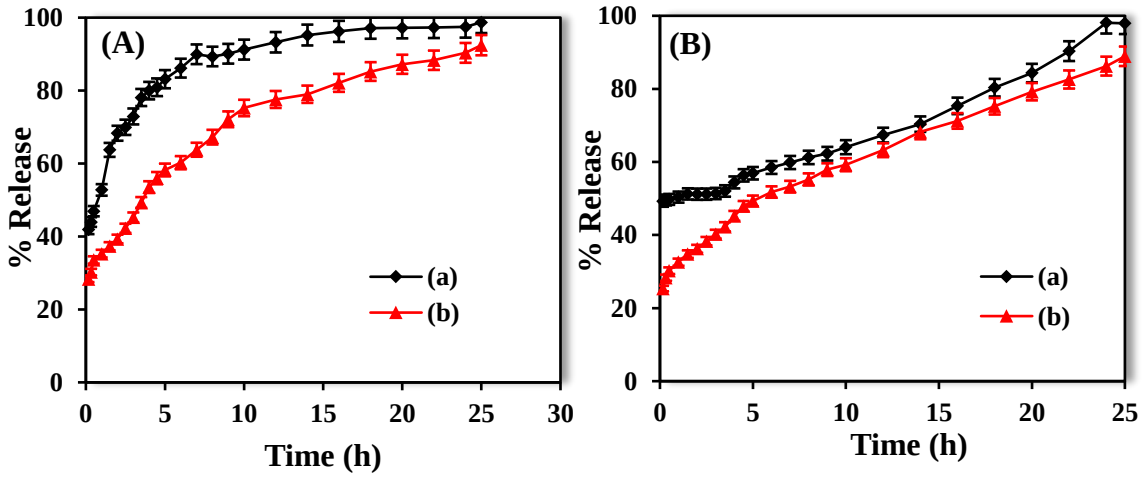

Figure 12. Comparison of release profile of (A) **a** Asp/Np-MCM-41 with **b** Asp/TPA-Np-MCM-41 and (B) **a** Cap/Np-MCM-41 with **b** Cap/TPA-Np-MCM-41

Further to check that TPA act as only functionalizing agent and its structure remain intact during release study, FTIR analysis of Asp/TPA-Np-MCM-41 and Cap/TPA-Np-MCM-41, after release study were also carried out and spectra are shown

in Figure 13. FTIR spectrum in both case is similar with Figure 3d (TPA-Np-MCM-41) which confirmed that structure of TPA remains intact in Asp/TPA-MCM-41 even after release study and it's truly act as functionalizing agent.

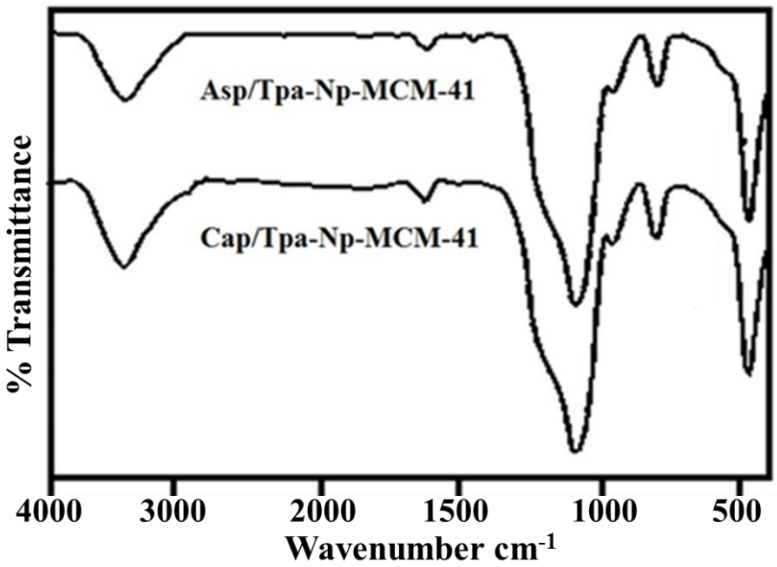

Figure 13. FTIR of drug loaded materials after release study

Kinetics and mechanism

In order to analyze drug release in a detail and obtain the possible release mechanism, release data up to 10 h is fitted with first order release kinetic model and Higuchi model.

(i) First order release kinetic model

First order release kinetic model is applied to study the dissolution of drug encapsulated in porous matrices. According to this model rate of release is concentration dependent. Figure 14 shows plot of Log of percentage remaining data against time. It was found that the release of Captopril as well as Aspirin follows the first order kinetic with linearity. Further, higher linearity and higher co-relation coefficient were obtained for Asp/TPA-Np-MCM-41 (R^2= 0.9929) and Cap/TPA-Np-MCM-41 (R^2= 0.9813).

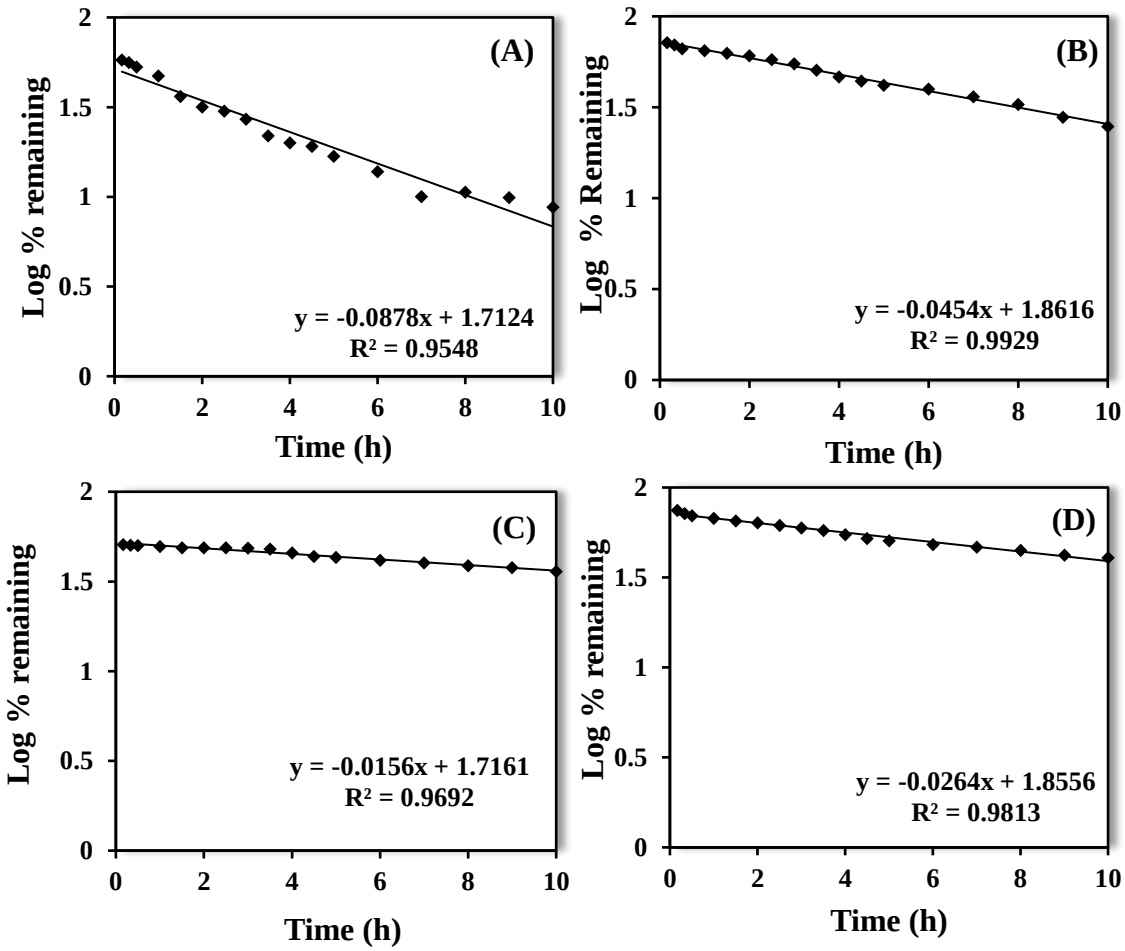

Figure 14. First ordered release kinetic model of (A) Asp/Np-MCM-41, (B) Asp/TPA-Np-MCM-41, (C) Cap/Np-MCM-41 and (D) Cap/TPA-Np-MCM-41

(ii) Higuchi Model

The Higuchi model (Figure 15) describes the percentage release versus square root of time dependent process based on fickian diffusion. The release mechanism of both drug is best explained by this model with high linearity and high correlation coefficient (R^2) value for Asp/TPA-Np-MCM-41 (R^2 = 0.9793) and Cap/TPA-Np-MCM-41 (R^2 = 0.991). Higher value of R2 for suggests, more ordered release of drugs from TPA-Np-MCM-41 as compared to pure Np-MCM-41. Thus kinetic and mechanistic study shows that drug release is concentration dependent process, follows first order release kinetics as well as it follows the Fickian diffusion mechanism.

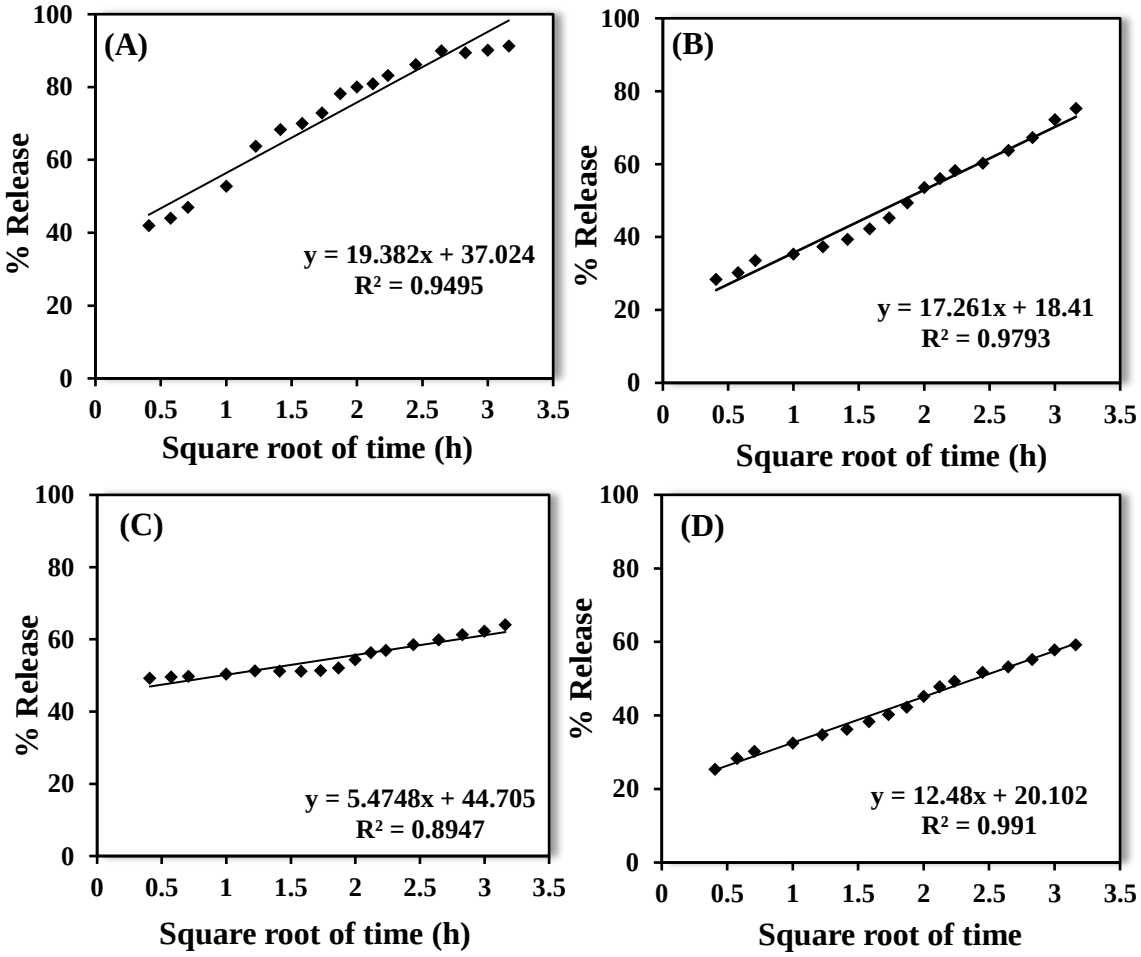

Figure 15. Higuchi Model of Asp/Np-MCM-41, Asp/TPA-Np-MCM-41, Cap/Np-MCM-41 and Cap/TPA-Np-MCM-41

Kinetic study also confirms that more ordered and controlled release profile were obtained from TPA-Np-MCM-41 as compared to pure Np-MCM-41.

Comparision of MCM-41 and Np-MCM-41

Table 2. shows a comparison of loading effeciency (LE) of MCM-41 and Np-MCM-41. Higher LE was obtained for Np-MCM-41 as compared to MCM-41 as former has higher specific surface area (1100 m^2/g) as compare to later one (890 m^2/g). Further, a comparision of release profile obatined for both drugs shows similar patren from MCM-41 as well as Np-MCM-41.

Table 2. Comparision of loading effecincy of MCM-41 and Np-MCM-41

Drugs	**Amount of drug mg/g of materials**	
	MCM-41	**Np-MCM-41**
Aspirin	52 ± 2	58± 2
Captopril	52 ± 2	67 ± 2

Conclusion

- Synthesis of Np-MCM-41 was carried out by non-hydrothermal synthetic method and functionalization was done by using wet impregnation method.
- Synthesis and functionalization of Np-MCM-41 was achieved successfully, and confirmed by elemental and spectral studies.
- Loading of L-Arginine was carried out by wet impregnation method and Loading of Aspirin/Captopril was carried out soaking method. Higher loading was observed for Np-MCM-41 as compared to TPA-Np-MCM-41.
- BET surface area analysis shows presence of L-Arginine/drugs molecules inside the channels of carrier.
- FTIR analysis shows the type of interaction present between the L-Arginine and carrier. From spectroscopic characterization, the possible interaction between the L-Arginine/drugs and carrier is mainly hydrogen bonding.
- Low angle powder XRD and TEM confirms uniform dispersion of L-Arginine/drugs inside the hexagonal mesoporous channels of carrier.
- In vitro release study of L-Arginine from Np-MCM-41 shows that L-arg_1/Np-MCM-41 is best system as compared to L-arg_2/Np-MCM-41 and L-arg_3/Np-MCM-41.
- Comparison of release profile of L-Arginine from Np-MCM-41 and TPA-Np-MCM-41 shows that L-arg_1/TPA-Np-MCM-41 is best systems.
- Comparison of release profile of drugs from Np-MCM-41 and TPA-Np-MCM-41 shows that drugs loaded into TPA-Np-MCM-41 are the best systems.
- In vitro release study of L-Arginine/drugs shows that under stirring condition, fast release was observed as compared to under static condition. Further, it shows pH has great influence on the release rate.
- Kinetic and mechanistic study shows that release profile of L-Arginine/drugs follows first order kinetic and Higuchi diffusion mechanism.

References

[1] Q. Cai, Z.S. Luo, W.Q. Pang, Y.W. Fan, X.H. Chen, F.Z. Cui, Chem. Mater. 13, 258 (2001).

[2] S. Kumar, S.B. Rai, Indian J. Pure Appl. Phys. 48, 251 (2010).

[3] M. Kruk, M. Jaroniec, Langmuir 15, 5279 (1999).

[4] H.Y. Zhu, X.S. Zhao, G.Q. Lu, D.D. Do, Langmuir 12, 6513 (1996).

[5] S. Kim, E. Marand, Micro. Meso. Mater. 114, 129 (2008).

[6] C. Rocchiccioli-Deltcheff, Inorg. Chem. 22, 207 (1983).

[7] G. Kamalakar, K. Komura, Y. Kubota, Y. Sugi, J. Chem. Technol. Biotechnol. 81, 981 (2006).

[8] Q. Fengyu, Z. Guangshan, L. Huiming, S. Jinyu, L. Shougui, Q. Shilun, J. Solid State Chem. 179, 2027 (2006).

[9] P. Horcajada, A. Ramila, J. Perez-Pariente, M. Vellet-Regi, Microporous Mesoporous Mater. 68, 105 (2004).

[10] J. Andersson, J. Rosenholm, S. Areva, M. Linden, Chem. Mater. 16, 4160 (2004)

[11] A. Ramilia, B. Munoz, J. Perez-Pariente, M. Vallet-Regi, J. Sol- Gel. Sci. Technol. 26, 1199 (2003).

Main Conclusions

- Synthesis, functionalization and characterization MCM-41 as well as MCM-48 by various physicochemical techniques have been carried out successfully.
- Based on in vitro release study and as well as kinetic and mechanistic study, we propose that soaking method is better as compared to wet impregnation for obtaining desire release rate.
- Further, the comparison of release profiles obtained from MCM-41 and MCM-48 suggests that carrier geometry has pronounced influence on release rate of amino acids/drugs.
- It also shows that stirring as well pH of the medium have effect on release rate depending on type of interaction present between amino acid/drug and carrier.
- Modification of the carrier using TPA slows down the release rate compared to pure one and this can increase the bioavailability of drug. This is further supported by in vivo release study of CPT/MCM-48 and CPT/TPA-MCM-48.
- Kinetic and mechanistic study shows that release of all amino acids/drug follows first order kinetic and Fickian diffusion mechanism.
- MTT study confirms that functionalization of carrier by TPA does not induce toxicity into the carrier.
- Based on MTT study, CPT/MCM-48 as well as CPT/TPA-MCM-48 was selected for in-Vivo study and obtained results show that the AUC of for both systems in rats were 9802.13 ± 30.2 and 1358.52±30.2 ng/Lh respectively, which was significantly higher as compared to that of pure CPT (187.80±58 ng/Lh).
- Comparison of MCM-41 and Np-MCM-41 as carrier shows similarity in the nature of release profiles obtained from both carriers. However, for latter case, higher loading of drug is observed.

Novelty of work

- Designing and development of drug delivery systems based on mesoporous silica which was functionalized by inorganic moiety (TPA)
- Release profile of L-Arginine/Cysteine has been studied from pure and functionalized carrier.
- In vitro release profiles of drugs (Captopril, Aspirin and Camptothecin) have been studied with detailed kinetics.
- In vivo release profile for CPT/MCM-48 and CPT/TPA-MCM-48 has been obtained with all pharmacokinetic parameters.

List of research Paper Published

[1] 12-tungstophosphoric acid functionalized MCM-41: synthesis, characterization and study of controlled in vitro release of L-Arginine, A. Patel, P. Solanki, J Porous Mater (2016) 23:1113–1123

[2] Cysteine and N-acetyl cysteine encapsulated mesoporous silica: synthesis, characterization and influence of parameters on In-vitro controlled release, S. Pathan, P. Solanki, A. Patel, J Porous Mater J Porous Mater (2017) 24:1105–1115

[3] In vitro release of L-Arginine and cysteine from MCM-48: a study on effect of size of active biomolecules on release rate, P. Solanki, A. Patel, J Porous Mater, (2018) 25:1489–1498.

[4] Encapsulated Mesoporous MCM-41 Nanoparticles: A Study on In Vitro Release as Well as Kinetics, P. Solanki, A. Patel, Adv. Porous Mater. (2018) 6, 80–88.

[5] Camptothecin encapsulated into functionalized MCM-41: In vitro release study, cytotoxicity and kinetics, P. Solanki, S. Patel, R. Devkar, A. Patel, Mater. Sci. Eng. C (2019) 98, 1014–1021.

List of additional papers

[1] Functionalized SBA-15 for controlled release of poorly soluble drug, Erythromycin, S. Pathan, P. Solanki, A. Patel, Microporous and Mesoporous Materials (2018) 258:114-121

List of papers presented at Conferences

[1] International conference on Frontier Research in Chemistry & Biology Interface, CDRI Lukhnow, February 25-28, 2015.

[2] National Seminar on Frontier areas in chemical science, The Maharaja Sayajirao University of Baroda, March 19, 2016.

[3] National seminar on Structures and Chemistry of materials, The Maharaja Sayajirao University of Baroda, October 15, 2016.

[4] XXXI Gujarat Science Congress, PDPU, Gandhinagar, February 4-5, 2017.

[5] International conference on recent advances on material chemistry, SRM, Chennai February, 14-18, 2017.

[6] Science Conclave, The Maharaja Sayajirao University of Baroda, February 28, 2017

[7] International conference on Nano and Functional Materials, BITS Pilani, Pilani Rajsthan, November 16-18, 2017 (Received award for best poster from RSC, Journal of Material Chemistry A).

[8] 24th ISCB International conference (ISCBC-2018) Frontier Research in Chemistry and Biology Interface, Jaipur Manipal University, January 11-13, 2018

[9] NCSTEA-2019 National conference on Novel chemical systems for Therapeutic and Energy Application, Sardar Patel University, vallabh vidhyanagar, 1-2, March 2019, (Received 1st Prize for oral presentation)